

## Article

# A Provenance Study of Upper Jurassic Hydrocarbon Source Rocks of the Flemish Pass Basin and Central Ridge, Offshore Newfoundland, Canada

Matthew Scott <sup>1,\*</sup>, Paul J. Sylvester <sup>2</sup> and Derek H. C. Wilton <sup>3</sup><sup>1</sup> Canada-Newfoundland and Labrador Offshore Petroleum Board, St. John's, NL A1E 1E2, Canada<sup>2</sup> Department of Geosciences, Texas Tech University, Lubbock, TX 79409-1053, USA; paul.sylvester@ttu.edu<sup>3</sup> Department of Earth Sciences, Memorial University of Newfoundland, St. John's, NL A1B 3X5, Canada; dwilton@mun.ca

\* Correspondence: mscott@cnlopb.ca

**Abstract:** A number of hydrocarbon discoveries have been made recently in the Flemish Pass Basin and Central Ridge, offshore Newfoundland, Canada, but there is only limited geological information available. The primary goal of this study was to determine the sedimentary provenance and paleodrainage patterns of mudstones and sandstones from the Upper Jurassic Rankin Formation, including the Upper and Lower Kimmeridgian Source Rock (organic-rich shale) members and Upper and Lower Tempest Sandstone Member reservoirs, in this area. A combination of heavy mineral analysis, whole-rock geochemistry and detrital zircon U-Pb geochronology was determined from cores and cuttings from four offshore wells in an attempt to decipher provenance. Detrital heavy minerals in 20 cuttings samples from the studied geologic units are dominated by either rutile + zircon + apatite ± chromite or rutile + apatite + tourmaline, with minor zircon, indicating diverse source lithologies. Whole rock Zr-Th-Sc trends suggest significant zircon recycling in both mudstones and sandstones. Detrital zircon U-Pb ages were determined in two mudstone and four sandstone samples from the four wells. Five major U-Pb age groups of grains were found: A Late Jurassic group that represents an unknown source of syn-sedimentary magmatism, a Permian–Carboniferous age group which is interpreted to be derived from Iberia, a Cambrian–Devonian group derived from the Central Mobile Belt of the Newfoundland–Ireland conjugate margin, and two older age groups (late Neoproterozoic and >1 Ga) linked to Avalonia. The Iberian detritus is abundant in the Central Ridge and southern Flemish Pass region and units containing sizable populations of these grains are interpreted to be derived from the east whereas units lacking this population are interpreted to be sourced from the northeast and possibly also the west. The Upper Tempest Sandstone contains Mesozoic zircons, which constrain the depositional age of this unit to be no older than Late Tithonian.

**Keywords:** sedimentary provenance; paleodrainage; Grand Banks; Newfoundland; hydrocarbon; Kimmeridgian source rocks; U-Pb zircon geochronology; heavy mineral analysis; automated mineralogy



**Citation:** Scott, M.; Sylvester, P.J.; Wilton, D.H.C. A Provenance Study of Upper Jurassic Hydrocarbon Source Rocks of the Flemish Pass Basin and Central Ridge, Offshore Newfoundland, Canada. *Minerals* **2021**, *11*, 265. <https://doi.org/10.3390/min11030265>

Academic Editor: Manuel Francisco Pereira

Received: 15 February 2021

Accepted: 2 March 2021

Published: 4 March 2021

**Publisher's Note:** MDPI stays neutral with regard to jurisdictional claims in published maps and institutional affiliations.



**Copyright:** © 2021 by the authors. Licensee MDPI, Basel, Switzerland. This article is an open access article distributed under the terms and conditions of the Creative Commons Attribution (CC BY) license (<https://creativecommons.org/licenses/by/4.0/>).

## 1. Introduction

The prolific Kimmeridgian hydrocarbon source rocks of the Grand Banks of Newfoundland have received considerable attention as they are the primary oil source rock for this significant petroleum district. The Egret Member, the Kimmeridgian source rock of the Jeanne d'Arc Basin has been studied in detail there, where there are four producing fields (Figure 1). Nearby basins, however, have only been studied to more limited degrees. The Flemish Pass Basin, in particular, has had significant hydrocarbon discoveries at the Mizzen area (2009), the Harpoon and Bay du Nord areas (2013), and the Bay de Verde and Baccalieu areas (2016). The region has been the focus for academic research as well [1]. The Flemish Pass Basin is separated from the Jeanne d'Arc Basin by a topographic high called the Central Ridge, in which hydrocarbon discoveries have also been made. Tithonian-aged

sandstone, consisting of four siliciclastic intervals interbedded with shale, is the primary oil reservoir at Mizzen [2]. The primary source for the oil is considered to be a Kimmeridgian organic-rich shale, likely equivalent to the Egret Member in the Jeanne d'Arc Basin [3]. Unlike the Jeanne d'Arc Basin, however, the source rock here is present as two distinct intervals, designated as the Upper and Lower Kimmeridgian Source Rock members of the Rankin Formation (Figure 2) [4,5]. Previous work on the Upper and Lower Kimmeridgian Source Rocks in the Flemish Pass has focused on organic geochemistry and hydrocarbon source potential of the units [6,7]. This study presents new mineral data that contribute to the understanding of this important interval within the basin. In addition to the Upper and Lower Kimmeridgian Source Rock members, the provenance of the entire Rankin Formation is investigated, including the interbedded Upper and Lower Tempest Sandstone members as well as intervals not assigned to a specific member. The Tempest sandstones have only been encountered in wells on the Central Ridge and are not well studied. Previous work has focused on the sedimentology and depositional environment [8–10]. As the Tempest sandstones are interbedded with the hydrocarbon source rock units, studying their provenance provides a more complete picture of drainage patterns during the Late Jurassic and adds a new dataset to better understand these potential reservoir sandstones.

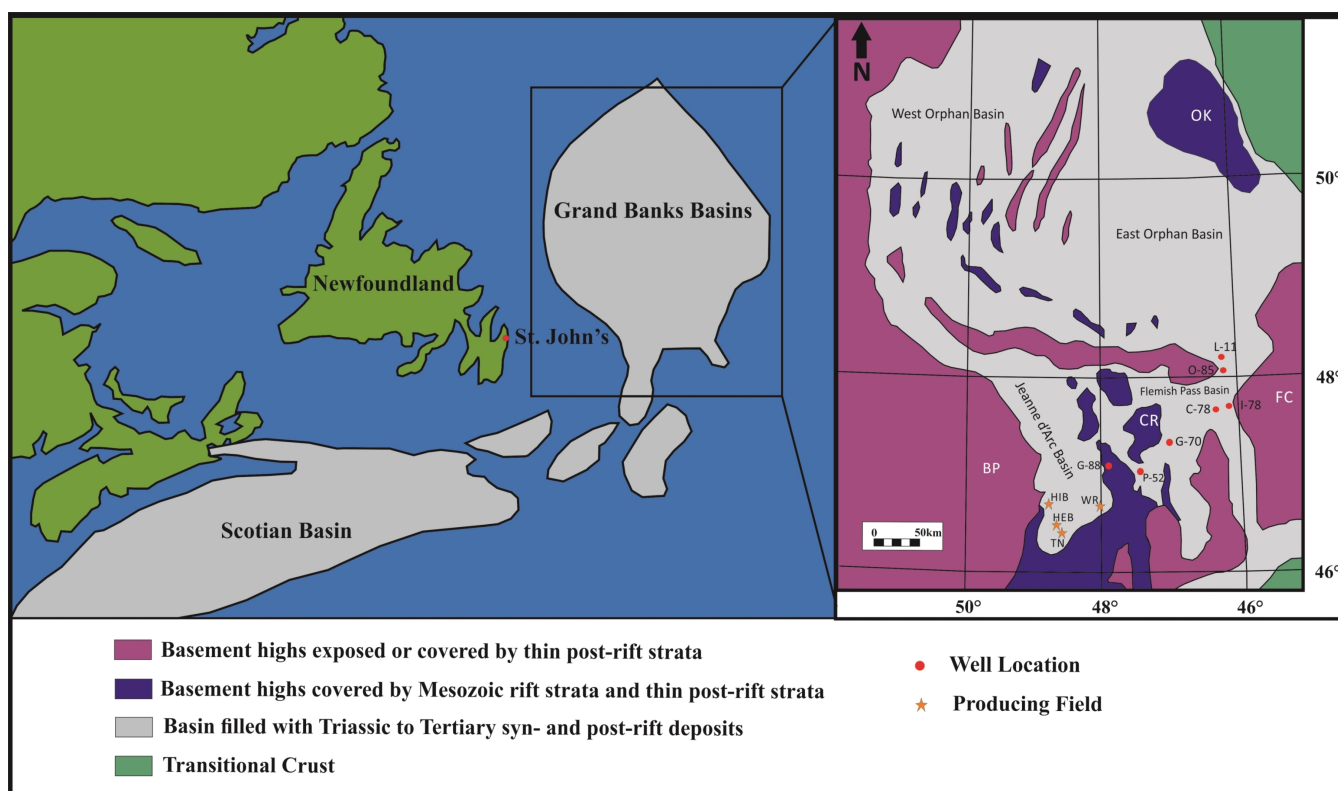


**Figure 1.** Regional location and geology of the Newfoundland Grand Banks. BP = Bonavista Platform; CR = Central Ridge; FC = Flemish Cap; OK = Orphan Knoll. Wells: P-52 = Panther P-52; I-78 = Baccalieu I-78; G-70 = Lancaster G-70; G-88 = South Tempest G-88; Mizzen L-11; O-85 = Harpoon O-85; C-78 = Bay du Nord C-78. Fields: HIB = Hibernia; HEB = Hebron; TN = Terra Nova; WR = White Rose. Well and field locations are approximate. Modified from Lowe et al. [1] and Enachescu [11].

The goal of this study is to determine the provenance and paleodrainage patterns during deposition of the Rankin Formation within the Flemish Pass Basin and Central Ridge. Lowe et al. [1] determined provenance patterns within the coarse-grained reservoir intervals of the basin using detrital zircon U-Pb geochronology as well as the geochemistry of detrital tourmaline. For this project, detrital zircon U-Pb geochronology, heavy mineral analysis and whole rock trace element geochemistry has been applied to determine provenance, with a focus on the finer-grained hydrocarbon source units. This enabled an

estimate of the areas where major drainage systems existed, and sediment supply was most abundant. All of the information gathered will enable a more accurate prediction of prospective areas for hydrocarbon exploration.

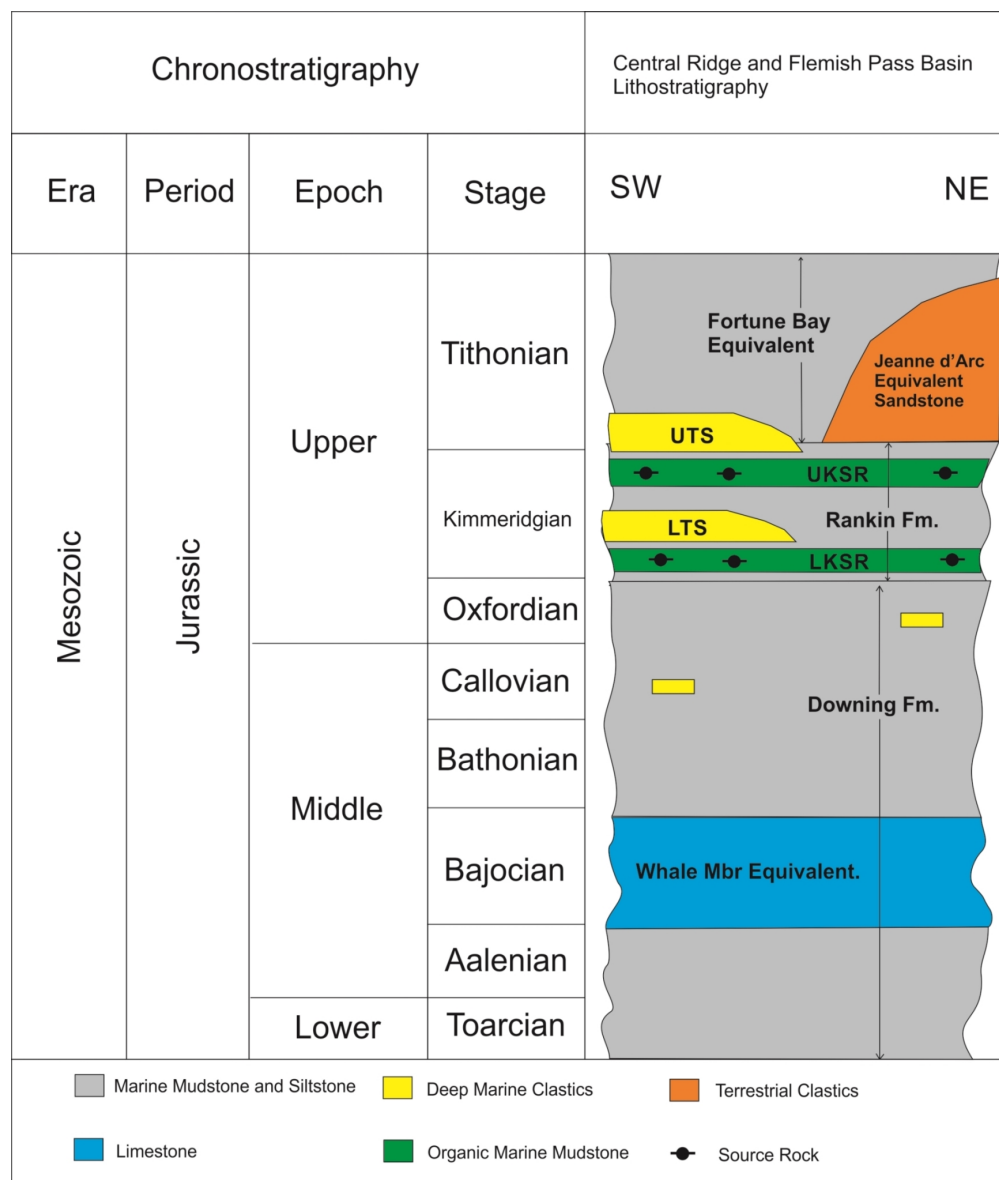


**Figure 2.** Stratigraphic chart for the Middle and Upper Jurassic in the Central Ridge and Flemish Pass Basin. UTS = Upper Tempest Sandstone; UKSR = Upper Kimmeridgian Source Rock; LTS = Lower Tempest Sandstone; LKSR = Lower Kimmeridgian Source Rock. Stratigraphic chart based on Sharp et al. [12], C-NLOPB [4,5].

## 2. Geological Setting

Mesozoic rocks of offshore Newfoundland are restricted to a series of northeast-trending rift basins. These basins are typically half-graben structures separated by Precambrian and Paleozoic basement highs and include the Jeanne d’Arc, Flemish Pass, East Orphan, and West Orphan basins (Figure 1). These Mesozoic basins were formed by rifting associated with the break-up of Pangea, spanning from the Permo-Triassic to the mid-Cretaceous [11,13,14]. Rifting progressed from south to north during the Late Triassic to the Early Cretaceous, which provided the conditions necessary for basin formation on the continental margin of Newfoundland. From the mid-Cretaceous to the present day, the evolution of the basins has been controlled by North Atlantic seafloor spreading and

passive margin sedimentation [11,13,14]. Of these basins, the Jeanne d'Arc Basin is the most prolific hydrocarbon province, with four producing fields.

Three rifting stages, interpreted to have affected sedimentation in many of the North Atlantic Basins [8,11], are clearly important in both the Flemish Pass and Jeanne d'Arc basins. The three rifting phases, according to Sinclair [8], include: (1) Triassic to Early Jurassic rifting during a period of NW-SE oriented extension, resulting in the break-up of Africa and North America; (2) Tithonian to early Valanginian rifting, during a period of E-W oriented extension, resulting in the break-up of Iberia and the Grand Banks; (3) Aptian-Albian rifting, during a period of NE-SW oriented extension, resulting in the break-up of Europe and North America. From the Late Cretaceous onwards, thermal subsidence was the dominant mechanism affecting the newly created continental margins. At this point, the Atlantic margin became a passive margin and hence associated passive margin sediments were deposited which continues to the present day.

### *2.1. Flemish Pass Basin Geological Overview*

The Flemish Pass Basin is located on the continental shelf of the Grand Banks approximately 400 km east of St. John's, Newfoundland (Figure 1). It covers an area of approximately 30,000 km<sup>2</sup> with water depths between 400 and 1100 m [15,16]. The basin is separated from the Jeanne d'Arc Basin to the southwest by the Central Ridge, bounded to the east by Beothuk Knoll and Flemish Cap basement high, to the north by the Cumberland High, and to the South by the Avalon Uplift [11,15,16] (Figure 1).

The oil and gas potential of the Flemish Pass Basin has been of great interest, particularly in recent years, as several large discoveries have been made and the existence of mature Upper Jurassic hydrocarbon source rocks, as well as the presence of potential reservoir units of Late Jurassic and Early Cretaceous age, has been confirmed. Additionally, industry 3-D seismic mapping has identified numerous significant structural traps, particularly some large faulted extensional anticlines [16,17]. In 2004, the Canada-Newfoundland and Labrador Offshore Petroleum Board (C-NLOPB) and the Geological Survey of Canada estimated that the Flemish Pass Basin contains 1.7 billion barrels of undiscovered petroleum resources (50% probability), with a range of field sizes from 528 to 44 million barrels [17].

Mature hydrocarbon source rocks of Kimmeridgian age were intersected in the Baccalieu I-78 well in the northern Flemish Pass. Rock-Eval analysis of samples from this well from McCracken et al. [6] defined total organic carbon (TOC) values from 0.92–4.83% (average 2.1%), and hydrogen indices (HI) ranging from 109–510 mg HC/g TOC (average 355 mg HC/g TOC), indicating type II, marine source rocks. Analyses of oil samples from sandstone reservoir intervals in Mizzen L-11 [3] and Gabriel C-60 [7] indicated the source rock possessed characteristics similar to the Egret Member of the Jeanne d'Arc Basin, with a likely more terrestrial component to the organic matter. Excellent reservoir quality sandstones were intersected in the Mizzen L-11 well into Upper Jurassic sandstones as well as 5 m of non-commercial oil pay in Cretaceous sandstone [18]. In 2009, StatoilHydro drilled the Mizzen O-16 well, and discovered 26 m of oil pay. Oil was found in the uppermost sand of the Tithonian, in a unit laterally equivalent to the Jeanne d'Arc sandstone of the Jeanne d'Arc Basin [2] (Figure 2). The Mizzen and Baccalieu areas are estimated to contain 102 and 45 million barrels of recoverable oil, respectively [19]. This discovery in the North Flemish Pass Basin has demonstrated the existence of a proven petroleum system, and Statoil has continued their evaluation of this system with a series of regional projects [2]. In addition to the O-16 well, Statoil made significant discoveries in both the Harpoon O-85 and Bay du Nord C-78 wells in 2013. In these wells, light, sweet oil was discovered in Tithonian fluvial sandstones [20]. The Bay du Nord and Harpoon areas are estimated to contain 407 and 40 million barrels of recoverable oil, respectively [19].

## 2.2. Central Ridge Geological Overview

The Central Ridge is a faulted intrabasinal high that separates the Jeanne d'Arc and Flemish Pass basins. The geological evolution of the Central Ridge is similar to that of the Flemish Pass Basin. Enachescu [11,13] stated that the Central Ridge was a relatively high area during the initial Late Triassic rifting episode. It was likely in a relatively elevated position until the late Jurassic [13]. Sinclair [8] demonstrated that the major appearance and uplift of the Central Ridge structure was predominantly Tithonian, and that this marks the initial isolation of the Jeanne d'Arc Basin from the northern Flemish Pass Basin. By the Early Cretaceous, the ridge reached its maximum elevation, and was exposed as an island chain or peninsula [13]. Since the island chain or peninsula was subaerially exposed, some of the Upper Jurassic and Lower Cretaceous sediments were eroded and are missing [13]. However, approximately 5 km of Upper Triassic to Upper Jurassic sediments remain a part of the succession at the Central Ridge [13].

There have been both oil and gas discoveries in the Central Ridge despite sparse drilling. Oil has been found in the South Tempest G-88 well, and gas at both North Dana I-43 and Trave E-87. High quality Kimmeridgian source rocks have been intersected in North Dana I-43, South Tempest G-88, and Panther P-52 and the ridge possesses a variety of structural trapping configurations [10,21]. These include tilted fault blocks, and inversion structures, in addition to a number of stratigraphic trapping possibilities [10]. Upper and Lower Tempest sandstone units are interbedded with shales and siltstones of the Upper and Lower Kimmeridgian Source Rock units (Figure 2). The Tempest sandstones are described as fine- to medium-grained sandstones interbedded with shales. They are interpreted as turbidite deposits [8–10] and flowed oil and gas at rates up to 1250 bbl per day and 4.9 mmcf per day, respectively, in the South Tempest G-88 well [4]. The North Dana I-43 well flowed 12 mmcf and 292 bbl per day of gas and condensate, respectively, from the equivalent Tempest sandstones [4]. The Tempest sandstones are interpreted as having been deposited from turbidity currents flowing to the north as structurally high areas exist to the South [10]. In addition to addressing the provenance of the Kimmeridgian hydrocarbon source rocks and associated Rankin Formation intervals, this study will also investigate the provenance of interbedded Tempest sandstones.

## 3. Sample Collection and Methods

Conventional cores and cuttings samples of Kimmeridgian hydrocarbon source rocks were collected from four wells from the study area. The wells chosen, Baccalieu I-78 and Lancaster G-70 from the Flemish Pass Basin, and South Tempest G-88 and Panther P-52 from the Central Ridge all intersected the Rankin Formation. The cores and cuttings were logged and sampled at the C-NLOPB Core Storage and Research Centre in St. John's, Newfoundland. Although samples from conventional cores were preferred for this study, the units of interest were not widely cored; thus cuttings, which were available from each of the four wells, were sampled where cores were unavailable.

Several different analytical methods were employed. For heavy mineral analysis, epoxy grain mounts from cuttings were analyzed on a scanning electron microscope using mineral liberation analysis techniques (hereafter referred to as MLA-SEM). For detrital zircon U-Pb geochronology, MLA-SEM imaging was followed by laser-ablation microprobe (LAM) ICP-MS analysis using both grain mounts and thin sections. Techniques employed for whole rock geochemical (major and trace element) analysis included X-Ray Fluorescence (XRF), and inductively coupled plasma-mass spectroscopy (ICP-MS). All sample preparation and analysis were done at Memorial University (St. John's, NL, Canada).

### 3.1. MLA-SEM Analysis

Two different methods were used to prepare samples for MLA-SEM analysis depending on whether the material in question was from core or cuttings. Where cores were available, it was only possible to obtain a small (5 cm × 3 cm × 3 cm) sample. With such a small sample, crushing and heavy liquid separation are not feasible as material would

likely be lost through the sample preparation process. Therefore, numerous polished thin sections were made from each small sample. Even where zircon was not abundant in the sample, there were enough grains identified to date zircon U-Pb ages by cutting several thin sections from the same interval.

For work on cuttings, approximately 50 g samples were available from the CNLOPB. The cuttings were taken from 5 m intervals and were received unwashed. The cuttings were gently disaggregated, cleaned, and wet sieved through a 15 µm mesh to remove the drilling mud and fine clays. This mesh size is considered appropriate because, for detrital zircon geochronology, the ability of the LAM-ICP-MS to analyze zircons smaller than 15 µm is limited by the sensitivity of the ICP-MS and thus the laser spot size. After the samples were cleaned, they were left to dry overnight and then sieved through a 180 µm mesh. This split the sample into two fractions: one 15–180 µm and the other >180 µm. The 15–180 µm split was then put through either the organic heavy liquid bromoform or a hydroseparator (CNT HS-11) to concentrate heavy minerals. For mudstone samples, the hydroseparator was used for heavy mineral separation because organic heavy liquids such as bromoform have been shown to be ineffective in clay-rich rocks [22,23]. For the sandstone samples, both heavy liquid separation using bromoform as well as hydroseparation were used. Bromoform and the sample were added to a separatory funnel which was carefully agitated to mix the bromoform and the sample. The heavies collected in the bottom of the funnel and were drained into an Erlenmeyer flask. The agitation, settling, and collecting process was repeated two more times. The heavy portion was then rinsed with acetone, and dried under a heat lamp. The hydroseparator produces heavy mineral concentrates using a controlled upward flowing, pulsating water stream. Based on the principles of Stokes' Law, light minerals are carried upwards in a glass separation tube while heavy minerals collect at the base of the tube. This methodology proved more effective than heavy liquids in the mudstone samples of this study. Once the heavy mineral concentration was completed, the sample was mounted in 25 mm epoxy rounds, left to cure overnight, and polished the next day.

Thin sections and grain mounts were imaged for heavy mineral grain abundance including zircon using the FEI MLA 650F SEM. The field emission SEM is equipped with an energy dispersive X-ray (EDX) detector, a backscattered electron (BSE) detector and Mineral Liberation Analysis software, which is capable of X-ray aided image analysis. The technique relies primarily on backscattered electron imaging (BEI) to define grain boundaries, and energy-dispersive X-ray (EDX) analysis, which classifies the grains as known mineral species. The MLA software has the ability to quantify mineral abundances, define associations of different mineral species, and define the sizes and shapes of minerals in a systematic fashion. Further details on the MLA-SEM system are available in Sylvester (2012) [24].

Typical instrument settings for MLA runs were: voltage set at 25 KeV, a beam current of 10 nA, a working distance of 13.5 mm, and a spot size of about 5.5 µm. Between 10,000 and 300,000 particles were identified and analyzed in each individual sample. Unknown mineral phases were identified based on matching their EDX spectra to that of EDX spectra of mineral standards (i.e., rutile, tourmaline, apatite, monazite, chromite, titanite, zircon). This is completed using the MLA Image Processing Tool software. Minerals of interest from the sample (particularly zircon) were imaged manually using the MLA Viewer Software. For detrital zircon geochronology, this permits the user to image and choose spots in the zircons that are optimal for age dating (i.e., free of inclusions, cracks, or other imperfections that could compromise quality of U-Pb analysis). The MLA outputs coordinates for the location of the imaged zircons within the thin section or grain mount.

A potential drawback of the MLA method in this study is the inability of the analytical equipment to differentiate between rutile and other TiO<sub>2</sub> minerals such as anatase and brookite. Therefore, MLA counts of rutile may also include some anatase and brookite. Additionally, rutile, brookite and anatase can all be found as authigenic phases and are common in sedimentary rocks [25,26]. The detrital TiO<sub>2</sub> minerals may be difficult to distinguish

from diagenetic phases as the detrital grains often have secondary porosity or inclusions. In addition, the authigenic grains may sometimes be fairly homogenous [25,26], particularly when dealing with fine grain sizes such as in this study. Textures of several rutile grains were analyzed in each sample but authigenic grains were not recognized. However, given the caveats mentioned, it is possible that authigenic  $\text{TiO}_2$  grains may be present. This is a consideration for the analysis of provenance based on heavy mineral ratios.

In addition to rutile, apatite can also form authigenically as noted by Pe-Piper and Weir-Murphy [27] and Lowe et al. [1]. The authigenic grains can be identified based on texture, and some representative apatite grains from each sample were analyzed to identify the presence of authigenic grains. A few samples were found to have grains with authigenic textures and these samples were excluded from the analysis.

There are several benefits of using the MLA-SEM for detrital zircon geochronology over traditional methods. Removing the need to manually pick zircon grains is a significant advantage, particularly in fine-grained rocks of this study where manually picking of tiny grains would be challenging. Additionally, in offshore settings such as the Newfoundland Grand Banks, there is often a scarcity of sample material. Using the MLA-SEM ensures that any grain that may be ideal for analysis is discovered, which allows the user to maximize the available material. Counts of number of grains, area % and wt.% for the most abundant heavy mineral species identified in the studied samples are listed in Table S1 of the Supplementary Materials.

### 3.2. Detrital Zircon Geochronology

LA-ICPMS U-Pb zircon geochronology was carried out using a Thermo-Scientific ELEMENT XR magnetic sector, single-collector ICPMS coupled to a Lambda Physik Compex Pro 110 ArF excimer GeoLas laser ablation system operating at a wavelength of 193 nm and a pulse width of 20 ns. The laser was operated at an energy density of 5–7 J/cm<sup>2</sup> and a repetition rate of 4–5 Hz, with a spot diameter of 20 micrometers. The sample aerosol was transported from the sample cell to the ICP using a He-carrier gas to reduce sample redeposition within the ablation cell, improving sample transport efficiency and resulting in more stable time-resolved signals.

Data acquisition for each analysis was about two minutes, with the first ~30 s used to measure the gas background followed by ~40 s of laser ablation, and ~50 s of wash out. Measurements were carried out in peak-jumping mode with one point measured per peak. Isotopes measured were <sup>200</sup>Hg, <sup>202</sup>Hg, <sup>204</sup>Hg+Pb, <sup>206</sup>Pb, <sup>207</sup>Pb, <sup>208</sup>Pb, <sup>232</sup>Th, <sup>235</sup>U and <sup>238</sup>U from both the zircon and gas background. Intensities for <sup>235</sup>U were calculated from <sup>238</sup>U assuming a natural, present-day <sup>238</sup>U/<sup>235</sup>U ratio (137.88), as the measured <sup>235</sup>U intensities for many analyses were low and thus had large uncertainties.

Raw data were dead-time corrected and reduced off-line using the Iolite 2.5 software [28] with the VizualAge DRS [29], which carries out background and signal interval selections, gas background subtraction, signal drift corrections, external calibration, and age and uncertainty calculations. The external calibration provides corrections for instrumental mass bias and laser-induced U/Pb fractionation. Common Pb corrections were ignored for all unknown zircons except those in sample Lancaster G-70 (4405 m), which had elevated <sup>204</sup>Pb count rates. In this sample, common Pb was calculated and subtracted using the method of Andersen (2002) [30] in VizualAge [29]. Signal intensities of zircon of unknown age and Th/U concentration ratio were calibrated against standard reference material 91500 zircon (1065 ± 3 Ma) [31]. Ages and 2-sigma uncertainties were calculated from the corrected <sup>207</sup>Pb/<sup>206</sup>Pb, <sup>207</sup>Pb/<sup>235</sup>U and <sup>206</sup>Pb/<sup>238</sup>U ratios. Age determinations were calculated using the decay constants of Jaffey et al. [32]. Final Concordia diagrams, U-Pb age histograms and probability density plots were produced using the Isoplot/Ex3.75macro [33]. U-Th-Pb LA-ICP-MS detrital zircon data for the studied samples are listed in Table S2A of the Supplementary Materials.

In order to monitor the efficiency of the instrumental mass bias and laser-induced fractionation corrections, standard reference materials, 02123 zircon ( $295 \pm 1$  Ma; [34]), Plešovice zircon ( $337.13 \pm 0.37$  Ma; [35]), 91500 zircon ( $1065 \pm 3$  Ma; [31]), and OG-1 zircon ( $3465.4 \pm 0.6$  Ma; [36]) were analyzed between every 8 unknown zircons during each analytical session. These standard measurements also provided an estimate of the accuracy and reproducibility of the U-Pb analyses. The weighted mean  $^{206}\text{Pb}/^{238}\text{U}$  age for all analyses of 02123 was  $294.63 \pm 0.8$  Ma ( $2\sigma$ , MSWD = 1.7;  $n = 203$ ), for Plešovice was  $342.4 \pm 1.6$  Ma ( $2\sigma$ , MSWD = 2.4;  $n = 85$ ), and for 91500 was  $1062.0 \pm 1.6$  Ma ( $2\sigma$ , MSWD = 0.78;  $n = 368$ ) over the course of all the U-Pb analytical sessions. The weighted mean  $^{207}\text{Pb}/^{206}\text{Pb}$  age for all analyses of OG-1 was  $3475.5 \pm 2.5$  Ma ( $2\sigma$ , MSWD = 1.7;  $n = 79$ ) over the course of all the U-Pb analytical sessions. U-Th-Pb LA-ICP-MS zircon data for the reference materials are listed in Table S2B of the Supplementary Materials. In this study, the  $^{206}\text{Pb}/^{238}\text{U}$  age was used for grains younger than 1.2 Ga. The  $^{207}\text{Pb}/^{206}\text{Pb}$  age was used for grains older than 1.2 Ga. Only grains that were concordant within 10% were accepted.

For detrital zircon geochronology, the aim is to analyze as many zircons as possible to reduce the probability of missing an age population. Fedo et al. [37] stated that analysis of 59 randomly selected zircon grains from a sedimentary rock that has a normal abundance of zircon grains reduces the possibility of missing an age population to 5%. Similarly, Dodson et al. [38] indicated at least 60 grains must be analyzed to reduce the possibility of missing an age population greater than 0.05 to 95%. However, Vermeesch [39] calculated that to be 95% confident that no age population greater than 0.05 has been missed, 117 grains must be dated. However, this assumes that the sample has a perfectly uniform age distribution where each age group has the same number of grains [39]. This type of distribution is uncommon in naturally occurring populations. Therefore, Vermeesch [39] proposed that if age populations are not uniformly distributed, it is sufficient to date 95 grains to be 95% confident no age population greater than 0.05 has been missed. Vermeesch [39] suggested that if fewer than 117 grains are dated per sample, the probability of missing at least one age fraction should be reported.

In this study, as many grains as possible were analyzed in each sample. However, since these samples are derived from core and cuttings from offshore wells, a limited amount of sample material is available. Where cuttings were used, only 50 g samples over 5 m intervals were available. Samples could have been combined to cover 10 m or greater intervals, but this would have resulted in lower resolution for the provenance analysis and was therefore avoided. In samples where fewer grains were analyzed, it is possible that only the major age peaks were detected. However, given that this is the first study of this nature on these Upper Jurassic units from offshore Newfoundland, the major age peaks will still provide unique datasets and important provenance information. For each sample, the probability that an age peak has been missed is noted as suggested by Vermeesch [39].

### 3.3. Whole Rock Geochemistry

Samples for X-ray fluorescence (XRF) were taken from conventional cores, which were preferable as cuttings samples may possess unknown levels of contaminants from drill bit shavings, drilling mud and/or cave-ins from overlying units. Sample preparation involved pulverizing the rock into a fine powder using the Siebtechnik grinding mill. Strict laboratory protocols were followed to prevent contamination throughout this process.

XRF analysis was completed using a Fisons/Applied Research Laboratories model 8420+ sequential wavelength-dispersive x-ray spectrometer which has the capability for quantitative determination of major and minor/trace elements. Pressed pellets were used to obtain a full analysis of all, major, minor and trace elements. For the preparation of the pressed pellets, approximately 9 g of rock powder was weighed and mixed with 2.7 g of wax binder. This mixed powder was then put in a Herzog Pellet Press and pressed at 276 MPa for 10 s. The final preparation step was baking the pellet at 90 °C for 15 min. The pressed pellet analysis for trace elements,  $\text{Fe}_2\text{O}_3$  and MnO was completed on a Bruker

S8 Tiger WDXRF using the Geo-Quant T package. Two geological reference standards (USGS SGR-1B-1 Green River Shale and SDO-1-1 Devonian Ohio Shale) were analyzed with each group of 13 samples to confirm accuracy and precision for the results. XRF data for major and minor/trace elements are listed in Tables S3 and S4, respectively, of the Supplementary Materials.

To obtain a more complete analysis of trace elements, particularly those that are below the detection limit of XRF, inductively coupled plasma mass spectrometer (ICP-MS) was also carried out. For introduction of the rock powders into the ICP-MS as solutions, samples were digested in acid before analysis. The analytical procedure was as follows: (1) Initial digestion of a 0.1 g sample aliquot using HF/HNO<sub>3</sub> (also boric and oxalic acids); and (2) the resultant solution was analyzed using ICP-MS correcting for matrix effects using the method of standard addition. Full details of the procedure are given in Jenner et al. [40]. If any sample material was not dissolved fully in HF/HNO<sub>3</sub>, it was treated with HCl/HNO<sub>3</sub>.

In some samples, some resistant phases, most notably zircon, may not always dissolve completely in acid. In these cases, Zr, Hf, and HREE values should be considered minimum concentrations. Thus, samples were also digested as a Na<sub>2</sub>O<sub>2</sub> sinter which provides more complete decomposition of refractory phases and complete recovery of Zr, Hf, and HREE concentrations. For quality control, SGR-1B-1, and SDO-1-1 were prepared and analyzed with the other samples for both ICP-MS methods. ICP-MS data for trace elements are listed in Table S5 (HF/HNO<sub>3</sub> acid digestion) and Table S6 (Na<sub>2</sub>O<sub>2</sub> sinter digestion), respectively, of the Supplementary Materials.

## 4. Results

### 4.1. Whole Rock Geochemistry

Whole rock geochemical analyses were completed on samples of Upper Jurassic rocks from the Central Ridge and Flemish Pass Basin. Both sandstone and mudstone beds of the Upper and Lower Kimmeridgian Source rock members were sampled as well as of the Lower Tempest Sandstone member. Additional interbedded samples of the Rankin Formation were also analyzed with the above-mentioned Members. Since a significant amount of core was available over the Late Jurassic interval, all samples were of conventional core.

To help ascertain the composition of the detrital source region(s) and determine provenance, trace element plots were examined. Typically, the distribution of trace elements such as Ti, Mn, Zr, Hf, Nb, Sn, Cr, Ni, V, Co, La-Lu, Y, and Sc are sensitive to the nature of their detrital source region [41]. These elements have short residence times in seawater and are less susceptible to mobilization during sedimentary processes [41].

Figure 3 indicates that detritus for these Upper Jurassic units was predominantly derived from an upper crustal or felsic terrane as both the mudstone (Figure 3A) and sandstone (Figure 3B) samples plot in close proximity to the average composition of the upper continental crust. It is difficult to say precisely where this average upper crustal detritus is derived. However, nearby terranes such as the Avalon Zone and Central Mobile Belt of the Newfoundland-Ireland conjugate margin represent likely detrital sources as they both possess abundant felsic volcanic rocks as well as sedimentary cover sequences.

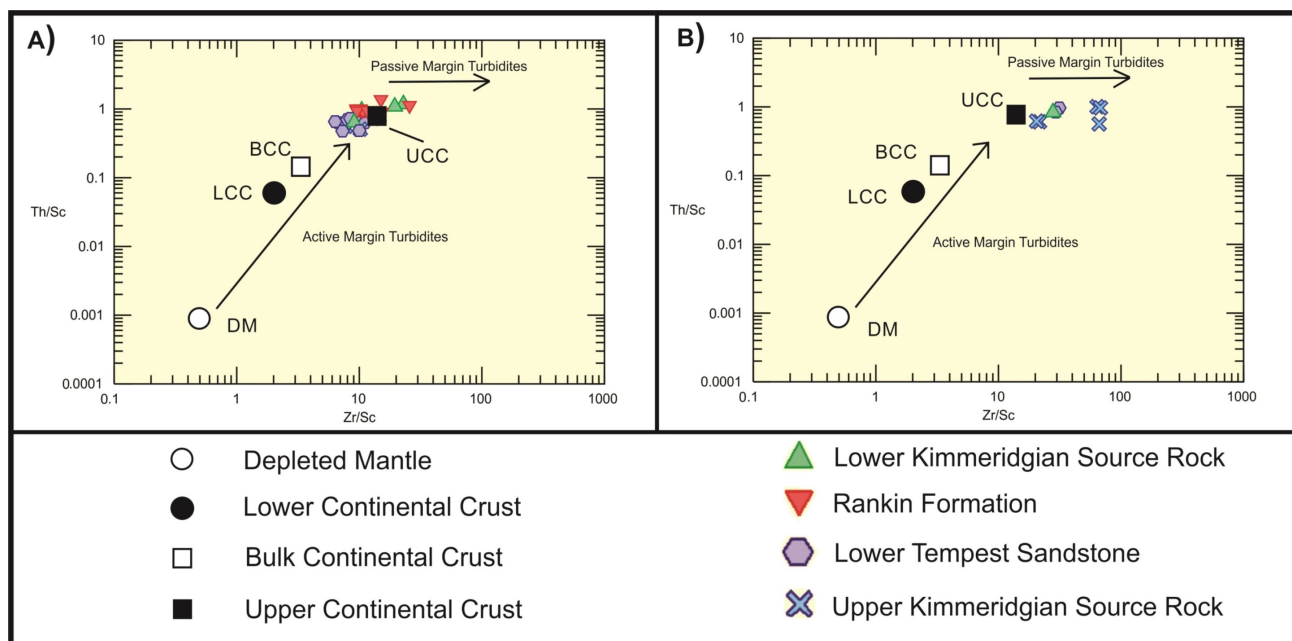


**Figure 3.** Zr/Sc vs. Th/Sc provenance diagrams for Upper Jurassic (A) mudstone and (B) sandstone samples. Figure from McLennan et al. [42].

The sandstone samples plot closer to the passive margin field than the mudstones as hydraulic sorting and sedimentary recycling processes acted to enrich the sand beds in recycled zircon. This indicates that the zircon in these beds is likely multi-cycle, and has been through multiple erosional and depositional cycles. However, the sandstones may not necessarily have had a different provenance than the mudstones, because recycling and enrichment of heavy minerals may have been more dominant in the sand-sized fraction of the detritus, which was not well sampled by the mudstones, which are biased to finer grains as a result of hydraulic sorting.

Samples from different stratigraphic units appear to have a similar provenance based on these plots. However, the Lower Tempest Sandstone samples plot slightly closer to the average composition of the Bulk Continental Crust. This suggests a slightly different provenance for the Lower Tempest Sandstone and that either felsic rocks or recycled sedimentary rocks were not as abundant of detrital sources for this unit compared to the others.

#### 4.2. Heavy Mineral Data

Methods for analyzing heavy minerals in this study follow the process outlined by Morton and Hallsworth [43,44]. This approach was applied by numerous authors to sandstones [1,45–47] as it employs detrital heavy mineral ratios to “fingerprint” the provenance of a given sample. This “fingerprint” is useful for correlation with provenance signatures from other units and to detect changes in provenance over time. It is necessary to use heavy minerals that are not significantly differentiated by hydraulic sorting during transport, and are not susceptible to dissolution during diagenesis. Minerals chosen for the analysis therefore have similar densities and are considered stable during burial diagenesis.

Typically, heavy mineral counts for conventional ratios are completed using a fine sand size bracket (63–177  $\mu\text{m}$ ) [1,43]. This grain size is typically chosen because within this range, all of the heavy minerals transported from the detrital source are considered to co-exist in the sedimentary deposit [43]. A 63–177  $\mu\text{m}$  size range is unsuitable for this study which includes fine-grained mudstones. Totten and Hanan [48] stated that the median size of heavy minerals in shales is approximately 25  $\mu\text{m}$  less than those found in sandstones. Therefore, placing the low end of the size bracket at 63  $\mu\text{m}$  would eliminate a significant portion of the heavy minerals in the samples studied. In Macquaker and Adams [49]

mudstone classification chart, they indicate a mudstone is any rock with >50% of the grains that are <63 µm. Understanding hydraulic equivalency [50], it is reasonable to expect heavy minerals within the mudstones and siltstones of this study to be significantly smaller than 63 µm. Therefore, the lower end of the size range used for these samples was 15 µm.

Heavy mineral counts were obtained from 20 cuttings samples from intervals of the Upper and Lower Kimmeridgian Source Rock, the Upper and Lower Tempest Sandstone and the interbedded Rankin Formation. Pie charts of the proportions of heavy minerals in a series of 13 representative samples are shown below in Figure 4. Of the 13 samples shown, seven are dominated by rutile (61–75% of the total heavy mineral count), zircon (8–17%) and apatite (7–17%), and three of the seven also contain significant amounts of chromite (5–10%). This heavy mineral assemblage is the most widespread among the samples, comprising the G-88 well in the Upper Tempest Sandstone, the I-78 and P-52 wells in the Upper Kimmeridgian Source Rock, the I-78, G-88 and G-70 wells in the Rankin Formation and the I-78 well in the Lower Kimmeridgian Source Rock. Thus, this heavy mineral assemblage is present in all of the units examined in this study except the Lower Tempest Sandstone.

A subordinate, heavy mineral assemblage dominated by rutile, apatite and tourmaline is found in four wells: the P-52 well in the Lower Tempest Sandstone and Lower Kimmeridgian Source Rock contains 30–41% rutile, 29–34% apatite and 19–27% tourmaline whereas the G-70 well in Upper and Lower Kimmeridgian Source Rock contains 66–71% rutile, 7–11% apatite and 10–11% tourmaline. Both types contain minor zircon (2–6%). This heavy mineral assemblage is present in all of the units examined in this study except the Upper Tempest Sandstone.

Two samples are anomalous with regard to their heavy mineral population: the sample from the P-52 well in the Upper Tempest Sandstone, which contains 61% zircon and 34% rutile, and that from the G-88 well in the Lower Kimmeridgian Source Rock, which contains 49% rutile, 23% apatite and 20% titanite.

Thus, in terms of heavy minerals, for geologic units analyzed from 3 or 4 wells, the Rankin Formation is most homogeneous, the Upper Kimmeridgian Source Rock somewhat more heterogeneous and the Lower Kimmeridgian Source Rock the most heterogeneous.

The heavy mineral populations of the various units of this study may also be described by the ZTR (zircon-tourmaline-rutile) index [51]. This index measures the percentage of zircon, tourmaline and rutile grains among all non-opaque and non-micaceous heavy minerals such as zircon, tourmaline, rutile, apatite, monazite, chromite, and titanite ( $ZTR = (Z + T + R) / (Z + T + R + A + Mz + Cr + Ti) \times 100$ ). The minerals in the denominator of the ZTR ratio are more susceptible to breakdown and dissolution during weathering and transport processes [44]. As the detritus is subject to progressively greater weathering and transport, it will become enriched in the more stable heavy minerals (chemically and mechanically) such as zircon, tourmaline and rutile compared to the unstable heavy minerals [51]. Therefore, this index is considered to be a reliable measure of sedimentary recycling [51]. This is the same principle as the Zr/Sc vs. Th/Sc plot shown in Figure 3 from the bulk rock trace element geochemical data.

One consideration for this study with respect to the ZTR index is that the minerals used in the denominator do not include all of the possible non-opaque, non-micaceous heavy minerals as in the standard definition of the ZTR index. The excluded minerals (such as epidote and olivine) are more unstable under diagenesis and were not included in the denominator of the ZTR index in this study. Since the dissolution of unstable phases and the variable nature of the effects of intrastratal dissolution are not well understood between these samples from different wells, it was important that only the diagenetically stable minerals listed above were used for this study. These minerals have been shown to be diagenetically stable up to depths of 4 km [44,52–54]. This allows for a reasonable comparison of maturity levels and contribution of first-cycle versus recycled detrital sources between samples.

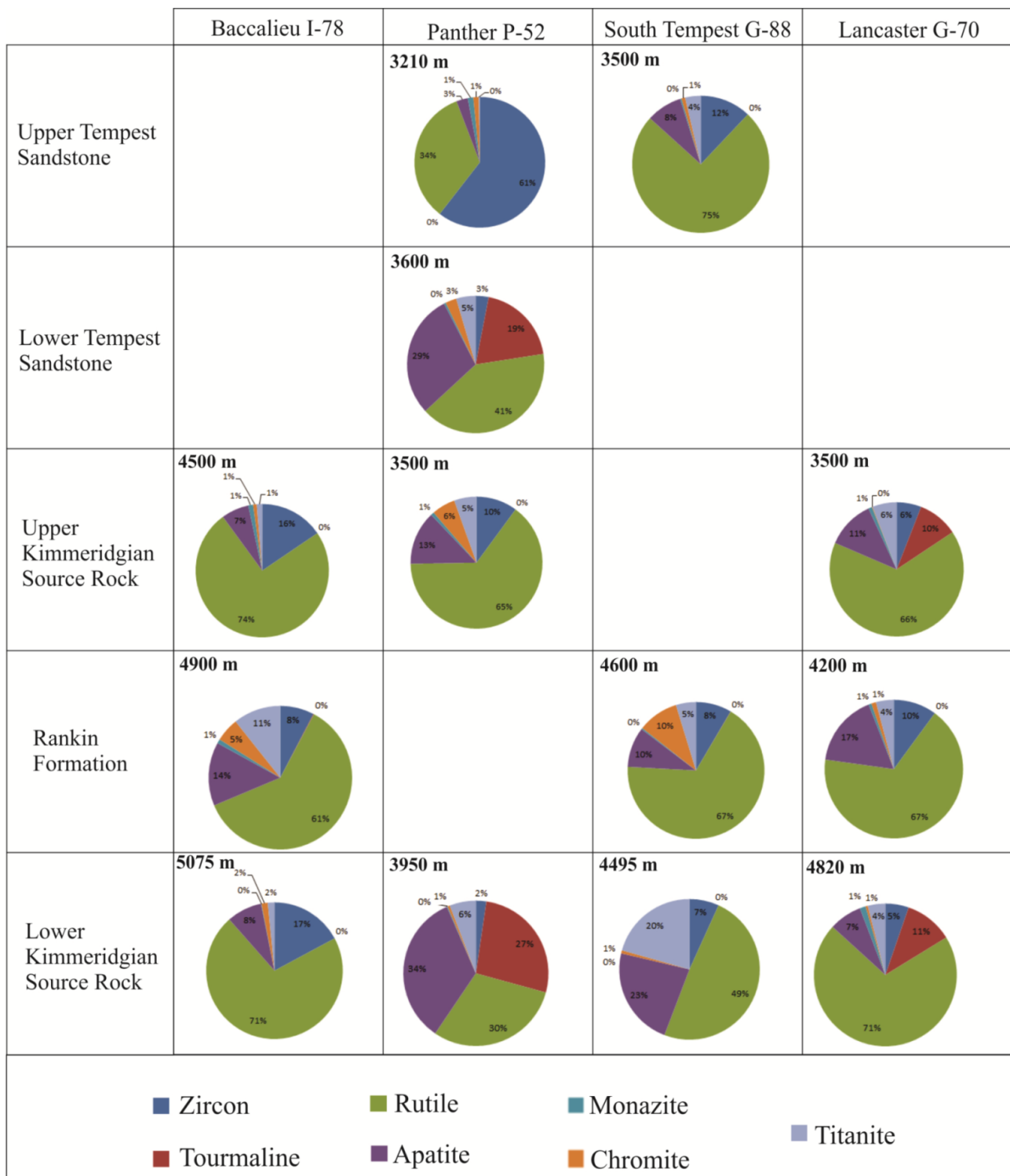


**Figure 4.** Pie charts of detrital heavy mineral proportions for Upper Jurassic samples from the Flemish Pass Basin and Central Ridge. Sandstone samples: I-78 (4500 m), P-52 (3210 m), P-52 (3600 m), P-52 (3500 m), G-88 (3500 m), G-70 (3500 m), G-70 (4200 m). Mudstone samples: I-78 (4900 m), I-78 (5075 m), P-52 (3950 m), G-88 (4600 m), G-88 (4495 m), G-70 (4820 m).

Two plots are shown below with the ZTR values for 20 samples from the various formations (Figure 5). Substantial heterogeneity is present for the Upper and Lower Kimmeridgian Source Rock units, while the Upper Tempest Sandstone and Rankin Formation samples are more homogeneous. Having only a single sample from the Lower Tempest Sandstone limits the significance of an interpretation of this interval. Overall, looking at the average values, it appears that most of the formations possess a similar average ZTR value in the range of 70–80. However, the average ZTR of the Upper Tempest Sandstone is slightly higher, at 85.

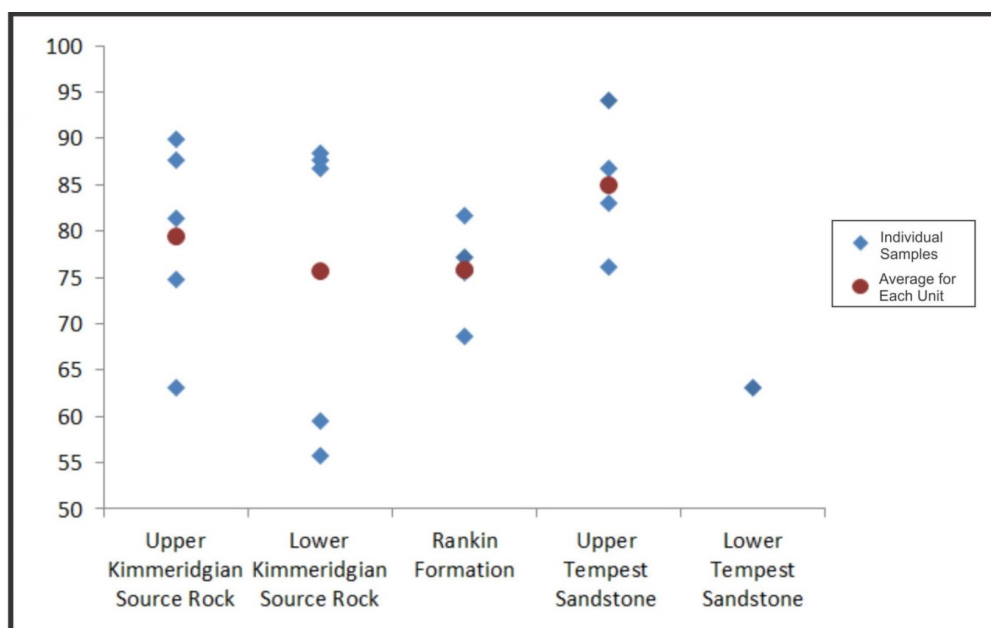


**Figure 5.** ZTR ratio plot for all Upper Jurassic samples from the Flemish Pass Basin and Central Ridge. Average heavy mineral index value from each formation also shown.

Overall, the detrital provenance of the Upper and Lower Kimmeridgian Source Rock and Rankin Formation appears to be broadly similar based on the ZTR values as well as a comparison of the heavy mineral pie charts. However, portions of the Upper Tempest Sandstone have slightly elevated ZTR ratios compared to the other studied units. This could indicate that sedimentary recycling was more significant in the Upper Tempest Sandstone samples, consistent with the unit containing a greater proportion of mature, zircon-rutile-rich coarse sandstone material than the 5 m cuttings intervals from the mudstone units (Kimmeridgian Source Rocks, Rankin Formation).

Only a single sample from the Lower Tempest Sandstone was analyzed. However, the sample does have an unusual heavy mineral signature, being rutile-apatite-tourmaline rich with a comparatively low ZTR ratio. This suggests an unusual provenance for this unit, consistent with the whole rock trace element plot presented in Figure 3B.

#### 4.3. Detrital Zircon U-Pb Geochronology

The geochronological analyses for this study were undertaken to define detrital zircon ages for mudstone and interbedded sandstone beds from the Upper Jurassic units. Six representative samples are discussed in the following section.

##### 4.3.1. Upper Kimmeridgian Source Rock

Several thin sections were prepared from a sample of conventional core from the Upper Kimmeridgian Source Rock at 3837.3 m depth in the South Tempest G-88 well. Although within the Upper Kimmeridgian Source Rock unit, this sample represents an interbedded sandstone bed and is defined as an arkosic wacke. Zircons from three thin sections were imaged using the MLA-SEM and then dated, yielding 56 concordant U-Pb

ages (Figure 6A) with three major populations. With 56 dated grains, using the method of Vermeesch [39], there is a 95% confidence that no fraction  $>0.10$  was missed. The first of the grain populations is a peak of 11 Cambrian–Devonian aged grains (533–405 Ma); the second group a major peak of 20 late Neoproterozoic-aged grains (626–544 Ma); and the third group is composed of 19 grains  $>1$  Ga (2740–970 Ma). Two smaller groups are also present. These are a Middle Neoproterozoic group of three grains (788–841 Ma), and two Permian–Carboniferous grains (281–341 Ma). One ungrouped grain is also present (941 Ma).

The Th-U ratios of the zircon vary from 0.11–1.24 (Figure 7A). The Cambrian–Devonian-aged grains have Th-U ratios ranging from 0.11–0.99, averaging 0.49. Grains from the prominent late Neoproterozoic peak have Th-U ratios ranging from 0.21–1.24 with an average of 0.62. and grains from the older,  $>1$  Ga group have Th-U ratios ranging from 0.21–1.01 with an average of 0.61. The Middle Neoproterozoic-aged grains have Th-U ratios ranging from 0.24–0.5 with an average of 0.36 while the two Permian–Carboniferous grains have Th-U ratios of 0.35 and 1.05, respectively. The single ungrouped grain has a Th/U of 0.36.

The key feature of grain morphology is also assessed for the dated grains from this sample (Figure 8A). Of all the grains, a subangular morphology was most common as 39% of all dated grains were subangular in shape. Five Cambrian–Devonian grains are subrounded, with four subangular, and two angular grains as well. Late Neoproterozoic grains are predominantly subangular (11 grains), with four angular grains, two subrounded grains, and three rounded grains. The group of  $>1$  Ga grains are composed primarily of subrounded grains (10 grains), with five rounded and four subangular grains present as well. Two of the Middle Neoproterozoic grains are subangular with one angular grain as well. The Permian–Carboniferous grains are both angular and the single ungrouped grain is rounded. Some representative grains of the various groups and their morphologies are shown in Figure 9.

Another sample of the Upper Kimmeridgian Source Rock was obtained from the Baccalieu I-78 well. The sample is a 5 m thick cuttings sample over the 4500–4505 m interval. Based on observations of the cuttings, this interval is composed of fine-grained mudstones with some interbedded siltstone. Grains were imaged using the MLA-SEM and 27 yielded concordant analyses (Figure 6B). With 27 dated grains, using the method of Vermeesch [39], there is a 95% confidence that no fraction  $>0.16$  was missed. The most abundant group of grains is late Neoproterozoic with 11 grains of this age present (552–661 Ma). Nine grains composed a group of Cambrian–Devonian grains (363–529 Ma). A small group of five grains  $>1$  Ga is also present. One Middle Neoproterozoic grain was dated (822 Ma) as well as one ungrouped grain of 949 Ma.

The Th-U ratios range from 0.10 to 1.05 (Figure 7B). The Cambrian–Devonian group of grains possess Th/U ranging from 0.18–1.05 with an average of 0.51. Grains from the prominent late Neoproterozoic peak have Th/U values from 0.41 to 0.99 with an average of 0.65, while grains from the  $>1$  Ga group have much lower Th/U with values ranging from 0.10–0.50 with an average of 0.29. The Middle Neoproterozoic grain has a Th/U of 1.05 and the ungrouped grain has a Th/U of 0.71.

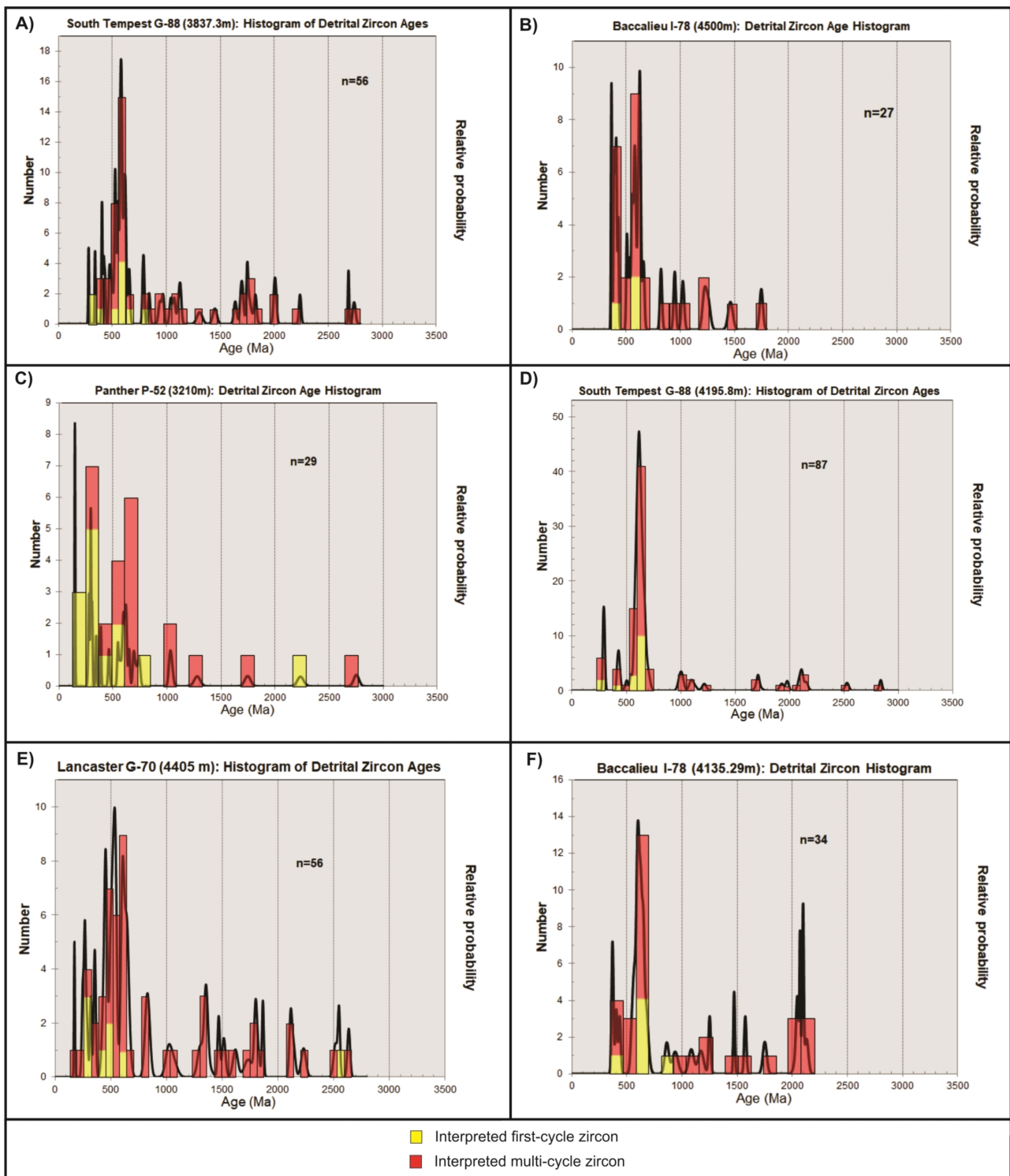


**Figure 6.** Detrital zircon age histograms (bars) and probability density plots (curves) for samples from four wells. The number of analyses shown includes only those that are concordant within 10%. Bin widths vary based on number of grains analyzed per sample. (A) Upper Kimmeridgian Scheme 88. (3837.3 m). (B) Upper Kimmeridgian Source Rock Mudstone cuttings sample from Baccalieu I-78 (4500 m). (C) Upper Tempest Sandstone cuttings sample from Panther P-52 (3210 m). (D) Lower Tempest Sandstone core sample from South Tempest G-88 (4195.8 m). (E) Rankin Formation Mudstone cuttings sample from Lancaster G-70 (4405 m). (F) Rankin Formation Sandstone core sample from Baccalieu I-78 (4135.29 m). First or multi-cycle zircon grains identified on the basis of grain morphology.

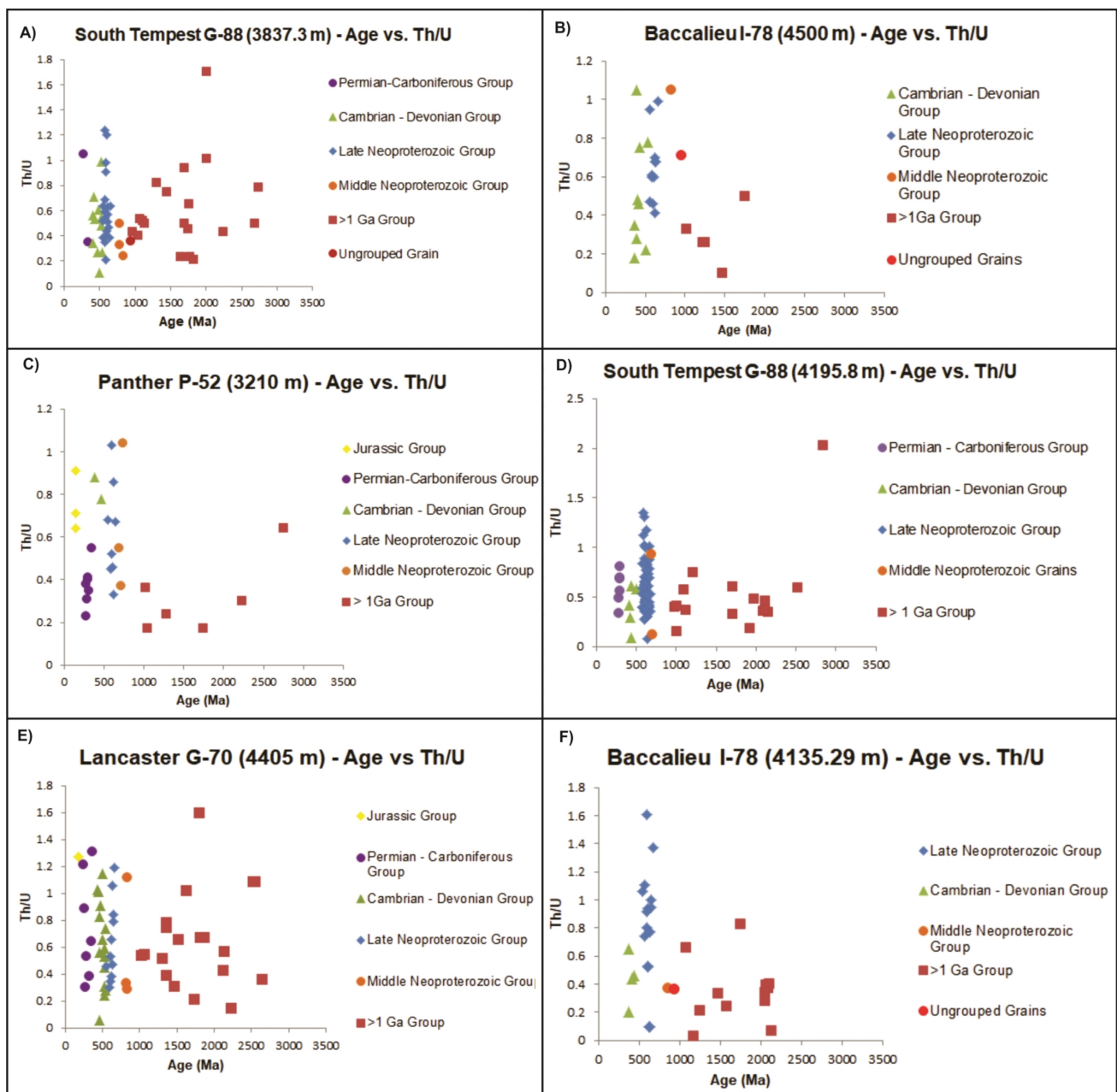


**Figure 7.** Age vs. Th/U graphs for samples from four wells. (A) Upper Kimmeridgian Source Rock Sandstone core sample from South Tempest G-88 (3837.3 m). (B) Upper Kimmeridgian Source Rock Mudstone cuttings sample from Baccalieu I-78 (4500 m). (C) Upper Tempest Sandstone cuttings sample from Panther P-52 (3210 m). (D) Lower Tempest Sandstone core sample from South Tempest G-88 (4195.8 m). (E) Rankin Formation Mudstone cuttings sample from Lancaster G-70 (4405 m). (F) Rankin Formation Sandstone core sample from Baccalieu I-78 (4135.29 m).

The morphology of all dated grains was also documented and may be the most important feature for determining the level of sedimentary recycling and/or the transportation distance (Figure 8B). Subangular grains are the most abundant type of grain making up 41% of all those dated. The Cambrian–Devonian group of grains is composed of mostly subangular grains with minor angular, subrounded, and rounded grains present as well. The late Neoproterozoic group of grains are also mostly subangular, however, subrounded and rounded grains are more important here than in the younger Cambrian–Devonian group. In the >1 Ga group of grains, the majority of grains are subrounded and rounded, with only one subangular grain. The Middle Neoproterozoic grain as well as the ungrouped grain are both subangular.

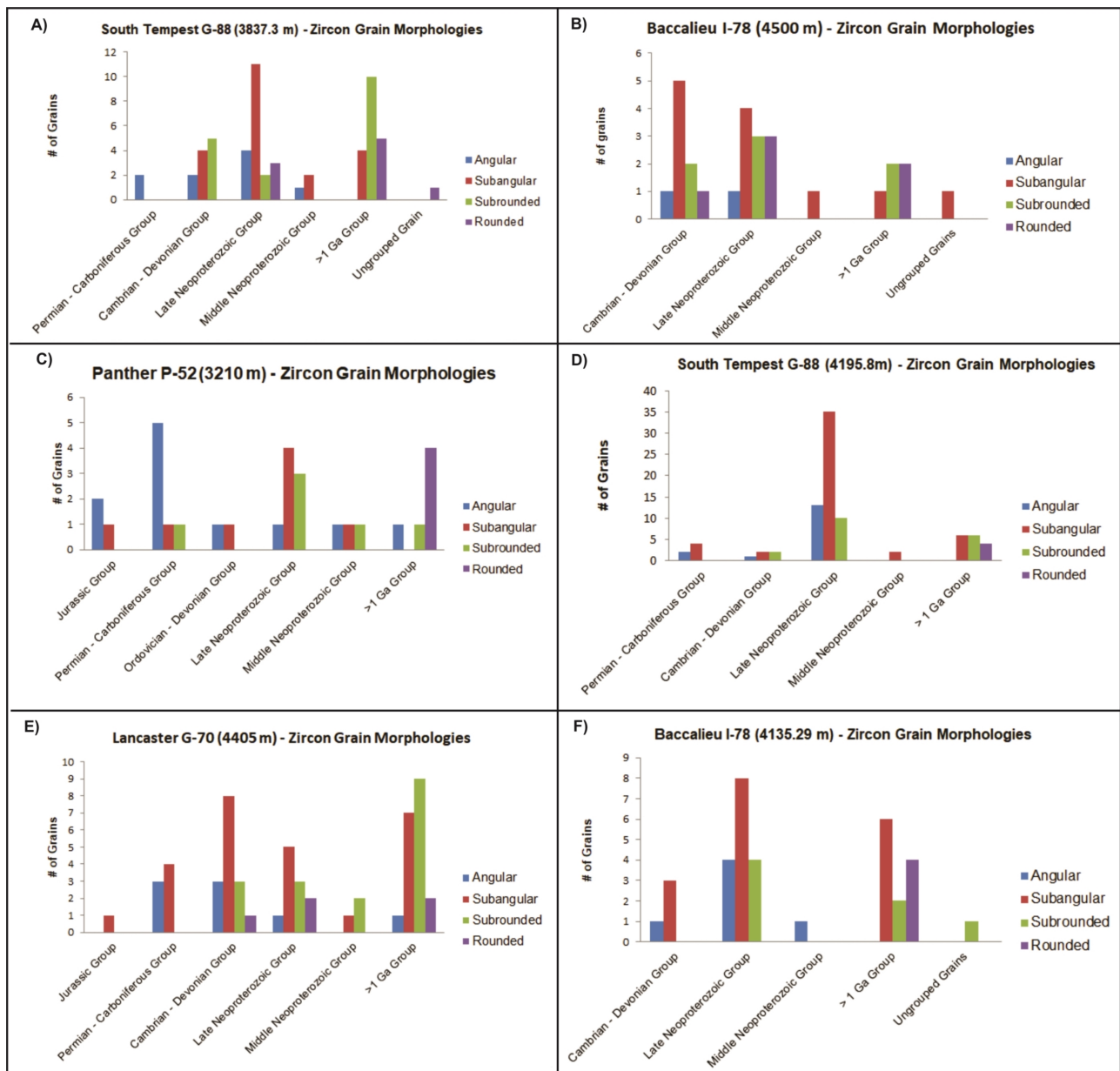


**Figure 8.** Histograms of zircon grain morphology for samples from four wells. (A) Upper Kimmeridgian Source Rock Sandstone core sample from South Tempest G-88 (3837.3 m). (B) Upper Kimmeridgian Source Rock Mudstone cuttings sample from Baccalieu I-78 (4500 m). (C) Upper Tempest Sandstone cuttings sample from Panther P-52 (3210 m). (D) Lower Tempest Sandstone core sample from South Tempest G-88 (4195.8 m). (E) Rankin Formation Mudstone cuttings sample from Lancaster G-70 (4405 m). (F) Rankin Formation Sandstone core sample from Baccalieu I-78 (4135.29 m).

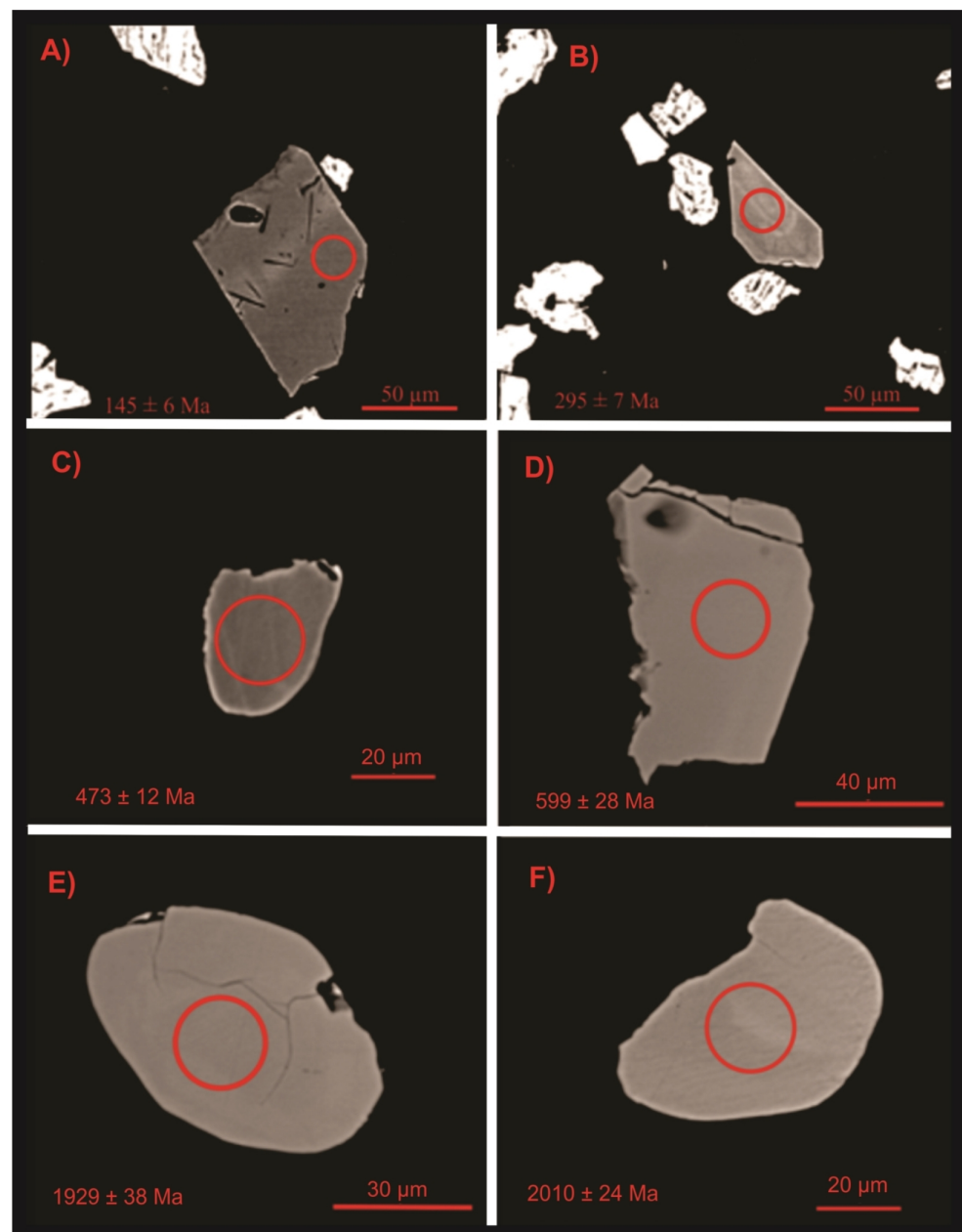


**Figure 9.** Images of detrital zircon grains from various Upper Jurassic samples. (A) Angular Jurassic grain in Upper Tempest Sandstone from Panther P-52 (3210 m). (B) Angular Permian grain in Upper Tempest Sandstone from Panther P-52 (3210 m). (C) Subrounded Ordovician grain in Upper Kimmeridgian Source Rock Sandstone from South Tempest G-88 (3837.3 m). (D) Subangular Neoproterozoic grain in Lower Tempest Sandstone from South Tempest G-88 (4195.8 m). (E) Rounded Paleoproterozoic grain in Lower Tempest Sandstone from South Tempest G-88 (4195.8 m). (F) Rounded Paleoproterozoic grain in Upper Kimmeridgian Source Rock Sandstone from South Tempest G-88 (3837.3 m). Red circle represents location grain was ablated.

#### 4.3.2. Upper and Lower Tempest Sandstone

A 5 m thick cuttings sample from the 3210–3215 m interval in the Upper Tempest Sandstone from the Panther P-52 well contained sufficient detrital zircons for analysis. Observations of the cuttings indicated that the interval was predominantly composed of fine-grained sandstone with some minor interbedded siltstones and mudstones. Grains were imaged using the MLA-SEM and 29 yielded concordant data (Figure 6C). With 29 dated grains, using the method of Vermeesch [39], there is a 95% confidence that no fraction >0.15 was missed. Five major groups of zircons are present. The most abundant is

the late Neoproterozoic group (545–649 Ma), with eight grains present. The next most abundant group consists of seven Permian–Carboniferous grains (275–345 Ma). Six older grains form a cluster of >1 Ga grains, ranging from 1026–2752 Ma. Another cluster is composed of three grains that are Late Jurassic in age (145–150 Ma). Three Middle Neoproterozoic grains are also present (691–743 Ma) as well as a final group of two grains that are Ordovician and Devonian, respectively.

Th/U of all concordant grains in this sample range from 0.17–1.04 (Figure 7C). The late Neoproterozoic grains possess values from 0.33–1.03 with an average of 0.63. The Permian–Carboniferous grains have values ranging from 0.23–0.55 with an average of 0.38. The >1 Ga grains have Th/U values ranging from 0.17–0.64 with an average of 0.31. The Jurassic grains possess higher Th/U values ranging from 0.64–0.91 with an average of 0.75. The Middle Neoproterozoic grains have Th/U values from 0.37–1.04 with an average of 0.65. The final group consists of two grains of Ordovician and Devonian age which possess high Th/U of 0.78 and 0.88 with an average of 0.83.

Of all concordant grains in the Upper Tempest Sandstone sample, the most common morphology is angular, as 38% of all grains possess this shape (Figure 8C). The late Neoproterozoic grains, however, are predominantly subangular (4 grains), with 3 subrounded and 1 angular grain. The Permian–Carboniferous grains, which are a new population not detected in previous samples, are predominantly angular (5 grains) with one subangular and one subrounded grain. These grains are a younger population, and the angular shape of the majority of these grains is evidence they have been subject to less attrition than some of the older populations. This can also be said for the Upper Jurassic grains, which are predominantly angular (2 grains), with one subangular grain. The >1 Ga grains are markedly different, as 4 of these grains are rounded, with 1 subrounded grain, and one angular grain. These grains have clearly been subject to more weathering and erosion than the other grains, as is evidenced by their predominantly rounded shapes. The Ordovician grain is subangular, while the Devonian grain is angular in shape. The Middle Neoproterozoic Group possesses one angular, one subangular and one subrounded grain.

A sample of the Lower Tempest Sandstone was obtained from a conventional core at 4195.8 m depth from the South Tempest G-88 well. The sample is a fine-grained sandstone. Zircons were mapped and imaged using the MLA-SEM. Of the imaged grains, 87 yielded concordant results (Figure 6D). With 87 dated grains, using the method of Vermeesch [39], there is a 95% confidence that no fraction >0.07 was missed. These grains fall into five major groups. The first is a group of 57 late Neoproterozoic grains (570–682 Ma). The second group is composed of 16 grains >1 Ga (986–2838 Ma) and the third group is a cluster of six Carboniferous–Permian grains (286–298 Ma). A group of six Cambrian–Devonian grains (416–541 Ma) as well as a small group of 2 Middle Neoproterozoic grains (696–707 Ma) are also present.

Th-U ratios of all concordant grains in this sample range from 0.08–2.03 (Figure 7D). The late Neoproterozoic grains possess Th/U values between 0.08–1.35 with an average of 0.61. The >1 Ga grains possess Th-U ratios ranging from 0.15–2.03 with an average of 0.53. The Permian–Carboniferous grains have Th-U ratios between 0.34–0.81 with an average of 0.60 and the Cambrian–Devonian grains possess Th-U ratios ranging from 0.09–0.61 with an average of 0.40. The two Middle Neoproterozoic grains have Th-U ratios of 0.93 and 0.12, respectively.

The most common grain morphology of all concordant grains in this Lower Tempest Sandstone sample is subangular, as 56% of the grains possess this shape (Figure 8D). The late Neoproterozoic grains are mostly subangular (34 grains), although 13 angular grains and 10 subrounded grains are also present. The >1 Ga grains are composed of six subangular, six subrounded and four rounded grains. As observed in previous samples, these grains tend to have more mature morphologies, indicating more attrition than the younger zircon groups. Of the six Permian–Carboniferous grains, four are subangular, while the other two are angular. The Cambrian–Devonian grains are composed of three

subangular grains, two subrounded grains, and one angular grain. The two Middle Neoproterozoic grains are both subangular.

#### 4.3.3. Rankin Formation

A 5 m thick cuttings sample from the 4405–4410 m interval from within the Rankin Formation was obtained from the Lancaster G-70 well. Observations from the cuttings indicated this interval was predominantly fine-grained, consisting of mudstones interbedded with minor siltstones and fine-grained sandstones. Unfortunately, many of the grains contained abundant  $^{204}\text{Pb}$ , and yielded discordant results. In this sample, of the 62 grains ablated, only 20 were less than 10% discordant. However, a common lead correction following the method of Andersen [30] was applied to the grains. After applying the correction, 56 of the 62 ablated grains plotted concordantly (Figure 6E) excluding one analysis with an anomalous age ( $112 \pm 5$  Ma), some 40 Ma younger than the established Late Jurassic biostratigraphic age of this interval as defined by Robertson Research [55]. Other biostratigraphic reports from Jenkins [56] and BP Exploration [57] also date this interval as latest Callovian to earliest Oxfordian (~160 Ma) and Early Kimmeridgian (~157 Ma), respectively. Since this sample is from drill cuttings, it is likely that this zircon grain was derived from higher in the stratigraphic section, from cavings of Cretaceous or younger strata. With 56 dated grains, using the method of Vermeesch [39], there is a 95% confidence that no fraction  $>0.10$  was missed. The grains define five prominent clusters. The youngest group is composed of seven Late Devonian–Permian-aged grains (361–248 Ma) (Figure 6E). Another group consists of 15 Cambrian to Silurian-aged zircons (545–431 Ma). A group of 11 late Neoproterozoic grains (664–548 Ma) is also present as well as a smaller group of three Middle Neoproterozoic grains (837–817 Ma). The largest and oldest group is composed of 19 grains with ages  $>1$  Ga (2636–1017 Ma). Additionally, one Upper Jurassic grain was dated at  $175 \pm 9$  Ma.

The Th/U of zircon grains from this sample range from 0.06–1.6 (Figure 7E). The Jurassic grain has a Th/U of 1.27. Th/U ratios are 0.3–1.31, with an average of 0.75 in the Late Devonian to Permian grains, 0.06–1.15 with an average of 0.62 in the Cambrian to Silurian grains, 0.3–1.19 with an average of 0.64 in the late Neoproterozoic grains, 0.29–1.12 with an average of 0.58 in the Middle Neoproterozoic grains and 0.15–1.60 with an average of 0.65 in the  $>1$  Ga grains.

The most common grain shape here is subangular, with 46% of the grains possessing this morphology (Figure 8E). The Jurassic grain is subangular, whereas the Late Devonian to Permian grains are characterized by three angular and four subangular grains. The Cambrian–Silurian grains possess a wide range of morphologies, with three angular, eight subangular, three subrounded and one rounded grain. The Late Neoproterozoic grains are characterized by one angular, five subangular, three subrounded, and two rounded grains. The Middle Neoproterozoic group is composed of one subangular and two subrounded grains. The group of  $>1$  Ga grains is predominantly subrounded (nine grains), with two rounded grains, seven subangular grains, and one angular grain.

A sample was obtained from conventional core in the Baccalieu I-78 well at 4135.29 m and is classified as an arkosic wacke. Thirty-four grains from this sample yielded concordant analyses (Figure 6F). With 34 dated grains, using the method of Vermeesch [39], there is a 95% confidence that no fraction  $>0.14$  was missed. The most abundant group of grains is late Neoproterozoic, and 16 grains of this age are present (546–683 Ma) (Figure 6F). The second most abundant group is the  $>1$  Ga grains, which is made up of 12 grains (1084–2130 Ma). A small group of four Silurian–Devonian grains is also present (370–404 Ma). Two other grains of  $862 \pm 37$  Ma, and  $938 \pm 52$  Ma were also dated.

Th/U of all dated zircon grains range from 0.02–1.61 (Figure 7F). The late Neoproterozoic grains possess values ranging from 0.02–1.61 with an average of 0.78. The  $>1$  Ga grains have values ranging from 0.03–0.83 with an average of 0.35. The Silurian–Devonian grains have values ranging from 0.2–0.65 with an average of 0.44. The grains of 862 and 938 Ma possess Th/U values of 0.37 and 0.36 respectively.

The most common grain morphology of all dated grains is subangular, as 50% of the grains possess this shape (Figure 8F). The late Neoproterozoic grains are mostly subangular (eight grains), although four angular grains and four subrounded grains are also present. The >1 Ga grains are predominantly subangular as well (six grains), although two subrounded and four rounded grains were also present in this group. The Silurian–Devonian grains are characterized by three subangular grains and one angular grain. The grain of 938 Ma is subrounded while the grain of 862 Ma is angular.

## 5. Discussion

### 5.1. Detrital Zircon U-Pb Age Groups

The most abundant zircon grains in the majority of the samples are late Neoproterozoic (~600 Ma), and these zircon are interpreted to have been derived from Avalon Zone rocks. Figure 10 demonstrates the similarity in detrital zircon age peaks between grains previously dated from the Avalon Zone [58] and from the late Neoproterozoic detrital zircon ages from this study. It is evident that the main detrital zircon peak seen in the data of Pollock et al. [58] matches nearly identically with the main late Neoproterozoic peak seen in grains from this study. In addition, data from other offshore Newfoundland samples from Lowe et al. [1] are plotted. These are also interpreted to be derived from Avalon Zone rocks, and also share the late Neoproterozoic age peak. Based on the grain morphologies as well as Th/U, these grains are likely derived from a mixture of recycled sedimentary rocks as well as plutonic and volcanic igneous rocks. This is consistent with a derivation from the Avalon Zone, as this terrane is characterized by volcanic and intrusive igneous rocks and associated sedimentary successions.

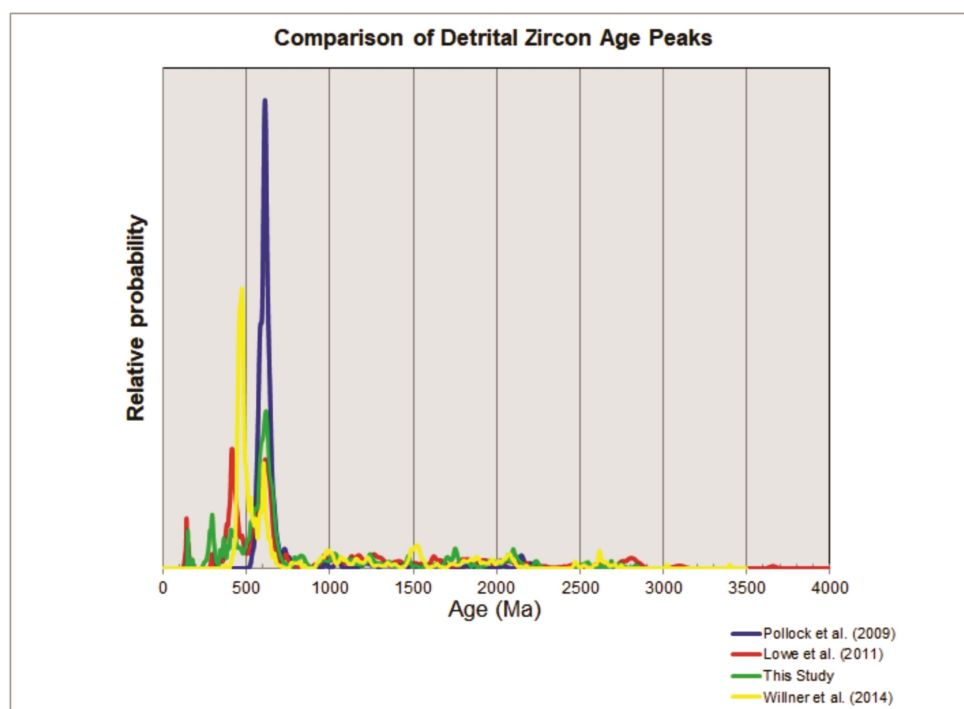


**Figure 10.** Comparison of detrital zircon age peaks from this study, Lowe et al. [1], Pollock et al. [58] and Willner et al. [59]. For this study, all concordant grains were plotted ( $n = 310$ ). All concordant grains from Lowe et al. [1] ( $n = 335$ ), Pollock et al. [58] ( $n = 278$ ) and Willner et al. [59] ( $n = 600$ ) were also plotted. Data from Lowe et al. [1] are from Mesozoic sedimentary rocks offshore Newfoundland while samples from Pollock et al. [58] are from Neoproterozoic to Cambrian sedimentary rocks of the Avalon Zone onshore Newfoundland. Data from Willner et al. [59] are from sedimentary rocks of the Central Mobile Belt onshore Newfoundland.

It is likely that the Avalon Zone was also an important detrital source for the group of grains of >1 Ga. Grains ranging from the Mesoproterozoic to the Late Archean are thought to be related to the basement of Avalonia. It has been proposed that the Avalon terrane is built upon a dominantly *c.* 1.0–1.2 Ga basement with a smaller component of *c.* 1.6 Ga crust [60,61]. Furthermore, rare *c.* 2.0 and 2.4 Ga xenocrystic zircons have been detected by Bevier and Barr [62] in the Mira terrane and Zartman and Hermes [63] in New England in Avalonian plutonic rocks. Therefore, it is possible the >1 Ga grains are derived directly from Avalon basement. However, these grains are also common in Avalon Zone cover sequences, especially within the Cambrian–Ordovician cover sequences [58]. These Lower Paleozoic cover sequences are thought to occur in the Avalon Uplift and Bonavista Platform areas, in addition to beneath the West Orphan, Northern Jeanne d’Arc and Flemish Pass Basins [64,65].

The characteristics of these grains, such as their low Th/U as well as their predominantly rounded to subrounded nature, were helpful in determining the parent rock type. It is probable that they were derived from a mixture of sedimentary and metamorphic detrital sources based on these features. This is reasonable because grains of this age would likely have experienced either significant sedimentary recycling or metamorphism. The rounded characteristic of these grains supports derivation from cover sequences of the Avalon Zone. >1 Ga grains from the Early Paleozoic cover sequences would have been subject to numerous sedimentary cycles, and would have many of the same features seen in the >1 Ga grains.

Another cluster of grains is a Cambrian–Devonian group, and these zircon are interpreted to be derived from Gander and Dunnage zone rocks in the Central Mobile Belt as the ages of these grains closely match those of rocks found in that region. As shown in Figure 10, the Cambrian–Devonian age peak from grains of this study closely matches that of Lowe et al. [1], suggesting the grains have a similar origin. Lowe et al. [1] also interpreted these grains to be derived from the Central Mobile Belt. Data from Willner et al. [59] from the Central Mobile Belt of Newfoundland are also plotted and show some correlation with the Cambrian–Devonian group from this study. There is an offset in the age peaks, as the main peak from Willner et al. [59] is slightly older than that of this study. However, this is explained by the data from Willner et al. [59] being from sedimentary rocks deposited prior to the emplacement of abundant Silurian–Devonian plutons in the Central Mobile Belt.

An additional consideration for the detrital source of the Cambrian–Devonian grains is that they may have been derived from Carboniferous sedimentary rocks. Abundant Carboniferous sedimentary rocks are present both in the Maritimes basins as well as on-shore and offshore Ireland. The St. Anthony Basin as well as the Sydney Basin both extend from northwestern and southwestern Newfoundland towards the east to the Northeast Newfoundland Shelf and the southern Grand Banks, respectively. Additionally, a number of wells on the southern Grand Banks intersected Carboniferous clastic sequences [65]. These Carboniferous sediments would probably be filled with Cambrian–Devonian-aged zircons as they most likely formed from the erosion of the Central Mobile Belt. This is the case for the Carboniferous clastic rocks of the Deer Lake and Bay St. George Basins of western Newfoundland which are dominated by zircons of Ordovician and Silurian age [66]. Carboniferous clastics deposited in the Clare Basin in Ireland also contain zircons in the Cambrian–Devonian age range eroded from rocks analogous to those of the Central Mobile Belt [67]. These clastics represent a potential detrital source, although the main zircon group in these samples is actually late Neoproterozoic [67]. The characteristics of the Cambrian–Devonian grains show a mixture of morphologies as well as variable Th/U. This indicates a mixture of parent rock types for these grains including both igneous and sedimentary detrital sources. Therefore, it is likely that rocks found within the Central Mobile Belt (Cambrian to Silurian sedimentary rocks, volcanic rocks, and Silurian to Devonian granites) are more important as a detrital source than the Carboniferous clastic rocks. If Carboniferous clastics were the predominant detrital source, there would likely be more rounded grains than what is observed for the Cambrian–Devonian grains, which were

often angular to subrounded. Although some of these are probably polycyclic, this can be explained from a derivation from sediments of the Central Mobile Belt.

Middle Neoproterozoic grains were dated in numerous samples but there are few known correlative detrital sources for grains of this age. A likely detrital source, however, is the Flemish Cap granodiorite, which is considered an offshore extension of the Avalon Zone. With an age in the 750–830 Ma range [68], it is located to the east and northeast of the Flemish Pass Basin.

Two other important age groups detected include the Permian–Carboniferous grains, as well as a group of Upper Jurassic grains. Permian–Carboniferous grains are noteworthy as there are few known correlative detrital sources from Newfoundland or the Newfoundland offshore. As shown in Figure 8, grains of this age were not detected by Lowe et al. [1] in other rocks from offshore Newfoundland. On the island of Newfoundland, there are some late Devonian intrusions such as the St. Lawrence Granite and Francois Granite, dated at  $374 \pm 2$  and  $378 \pm 4$  Ma, respectively [69]. However, no Permian–Carboniferous igneous rocks have been observed. If they did exist, they were either eroded, or are just very uncommon. However, even if Carboniferous igneous rocks were present in Newfoundland, it is unlikely that they would make statistically significant detrital zircon populations in offshore sediments, as Avalon, Gander, and Dunnage Zone related grains would be much more abundant. Additionally, if Carboniferous igneous rocks existed in Newfoundland, it is likely that the Carboniferous sedimentary rocks on the island would have a population of Carboniferous zircon grains. Sylvester [66] found no Carboniferous detrital zircon grains in the sedimentary rocks of the Deer Lake or Bay St. George Basins. Therefore, the presence of a sizable population of Carboniferous–Permian grains implies a detrital source external to Newfoundland.

Our preferred interpretation for the presence of Permian–Carboniferous zircons found in these samples is that they were derived directly from Iberia. Permian–Carboniferous granitic intrusions are abundant on the Iberian Peninsula [70], and therefore, detritus of this age would be abundant if the Iberian Peninsula represented a significant detrital source. Another possibility is that these grains represent second cycle detritus and are derived from recycled sediments of the Hercynian foreland basin. Hiscott et al. [71] preferred this interpretation to explain the presence of Permian–Carboniferous aged detrital micas within post-rift sediments in the Newfoundland Basin, east of the Grand Banks. However, the predominantly angular to subangular morphologies of the zircon grains within the samples of this study (Figure 8C–E) support a derivation as first-cycle detritus from a plutonic detrital source such as the Iberian granites as opposed to being derived from recycled sedimentary rocks.

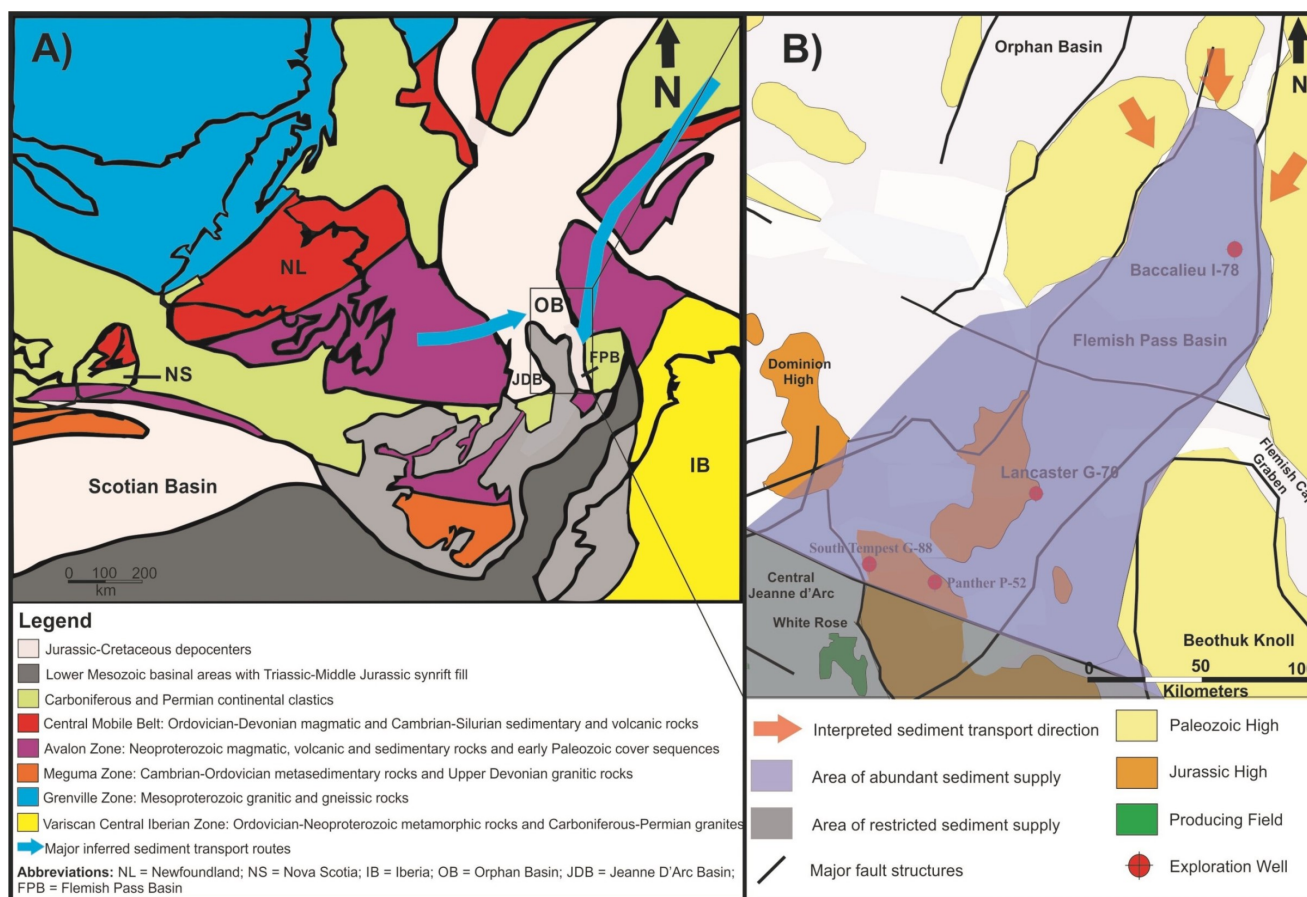
The provenance of the Upper Jurassic grains is difficult to identify as they have few known correlatives. Some potential Mesozoic detrital sources exist offshore Newfoundland, as well as on the island of Newfoundland. However, it is also possible that they are from a currently unknown detrital source of contemporaneous magmatism. The high Th/U as well as angular shapes of these grains indicate they are likely derived from igneous detrital sources, and are first-cycle in nature.

## 5.2. Paleodrainage Model–Upper and Lower Kimmeridgian Source Rock

This section provides an overview of the proposed drainage model for the Upper and Lower Kimmeridgian Source Rock members based on the zircon age-dates as well as whole rock geochemical signatures and heavy mineral analysis. The detrital zircon groups from the Upper Kimmeridgian Source Rock were characterized by detritus related to Avalonia (late Neoproterozoic, >1 Ga grains), detritus from the Central Mobile Belt (Cambrian–Devonian grains) as well as detritus linked to the Flemish Cap (Middle Neoproterozoic grains). The whole rock geochemical signatures also suggest an upper crustal provenance for the Upper Kimmeridgian Source Rock from rocks such as the Avalon Zone or Central Mobile Belt. Although no detrital zircons were analyzed from the Lower Kimmeridgian

Source Rock member, this unit shared the same geochemical fingerprint and is interpreted to have the same sediment sources.

It is difficult to determine conclusively the direction from which the dated detrital zircon grains were derived, as both Avalon Zone and Central Mobile Belt rocks exist west and northeast of the study area. It is possible that both areas were supplying detritus and this is shown in Figure 11A. The presence of detritus interpreted to be from the Flemish Cap granodiorite or correlative sequences, however, suggests that sediment input was at least in part from the northeast for these units. It is likely that basin entry points existed to the northeast, as interpreted by Cody et al. [2] for Upper Jurassic reservoir units of the Flemish Pass Basin. Figure 11A shows the interpreted large-scale drainage routes and Figure 11B shows the interpreted basin-scale entry points and areas of abundant and restricted sediment supply. In addition, much of the detritus in these samples is multi-cycle, as evidenced by both the Th/Sc–Zr/Sc plots (Figure 3) and the morphology of the detrital zircon grains (Figure 6A,B, and Figure 8A,B). Thus, sedimentary recycling was an important process in the deposition of these units.



If sediment was derived from the northeast, this implies sediment supply would have been much more abundant in the northern regions of the basin, with a likely thicker hydrocarbon source rock sequence. This is an important consideration for the petroleum potential of the source rock. If the hydrocarbon source rock is indeed more proximal to sediment supply in the north, then it is likely that it has a more terrestrial component in this region.

### 5.3. Paleodrainage Model—Upper and Lower Tempest Sandstones

The proposed drainage model for the Upper and Lower Tempest Sandstone members is based on the zircon age-dates as well as whole rock geochemical signatures and heavy mineral analysis. When the major zircon groups of the Tempest Sandstone samples are compared to those of the Upper Kimmeridgian Source Rock samples, it is clear they possess a different provenance. Permian–Carboniferous grains as well as Jurassic grains are found in the Tempest Sandstone samples, but are absent in the Upper Kimmeridgian Source Rock samples. Additionally, the Cambrian–Devonian group of grains is much more sparse in the Tempest Sandstones. The difference in morphology between zircon grains from the Tempest Sandstones versus those of the Upper Kimmeridgian Source Rock is also noteworthy. There are significantly more angular grains found in the Tempest Sandstone samples. The whole rock Th/Sc–Zr/Sc signature of the Lower Tempest Sandstone (Figure 3A) as well as heavy mineral assemblage of at least part of the Upper and Lower Tempest Sandstone (Figures 4 and 5) is also unique compared to the other studied units. The combination of these elements all suggests a different provenance for the Tempest Sandstone units. In contrast to the Upper and Lower Kimmeridgian Source Rock, the Tempest Sandstone units are interpreted to be derived from the east. The main driver for this is the presence of Permian–Carboniferous grains which are interpreted to be derived from Iberian granitic intrusions to the east. The lack of Cambrian–Devonian aged grains in the Tempest Sandstone samples likely also supports an easterly provenance. If there was a predominantly westerly provenance at this time, a larger population of Cambrian–Devonian grains would be expected, as was seen in samples from Lowe et al. [1] (Figure 10), who interpreted a westerly provenance in younger reservoir units in the Flemish Pass Basin.

As the Tempest Sandstone units are important reservoir intervals on the Central Ridge (flowed 1250 barrels of oil per day in the South Tempest G-88 well), the drainage orientations and basin entry points have important implications for reservoir quality during this time. Presumably, accumulations of coarse-grained, high quality reservoir rocks are more likely to occur in close proximity to sediment supply and basin entry points whereas finer-grained shales would be deposited basinward. If this is applied to the current interpretation for the Tempest sandstone, it is likely that higher reservoir quality rocks would have been deposited in the east, with decreasing reservoir grade to the west (Figure 12). This may be an important consideration for further exploration and drilling in this area.

### 5.4. Paleodrainage Model—Rankin Formation

Samples from the Rankin Formation were taken at various stages of the Upper Jurassic section and are broadly called Rankin Formation samples as they are not assigned to a specific member in the established stratigraphy [4,5] (Figure 2). The whole rock Th/Sc–Zr/Sc systematics and heavy mineral assemblages of the Rankin Formation samples are similar signatures to those of the Upper and Lower Kimmeridgian Source Rock units. However, the major zircon groups found in the Rankin Formation samples show different results. One sample from Baccalieu I-78 (4135.29 m) possesses very similar age peaks to the Upper Kimmeridgian Source Rock samples, with abundant grains related to Avalonia, as well as grains derived from the Central Mobile Belt. Conversely, the Rankin Formation sample from Lancaster G-70 (4405 m) has a detrital zircon age distribution that more closely matches that of the Tempest Sandstone samples from the Central Ridge. It is therefore interpreted that drainage patterns during deposition of the Rankin Formation were at times from the northeast (Figure 11), similar to the Upper Kimmeridgian Source Rock and at times from the east, comparable to the Tempest Sandstones (Figure 12). Eustatic changes or changes in the hinterland such as climate, uplift and erosion likely controlled which region was the primary sediment source.

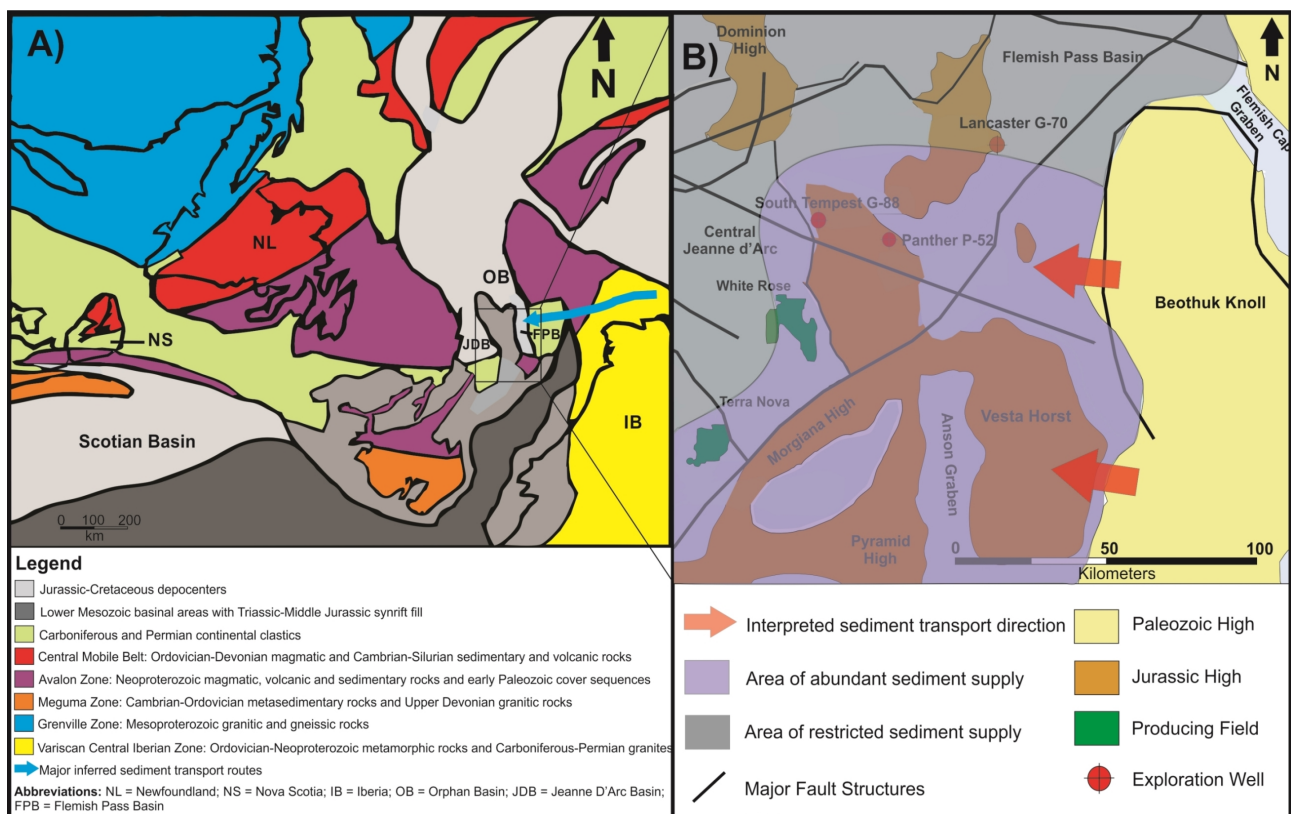


**Figure 12. (A)** Interpreted large scale drainage routes during deposition of the Upper and Lower Tempest Sandstone. Figure modified from Lowe et al. [1]. **(B)** Interpreted basin entry points and areas of abundant and restricted sediment supply during deposition of the Upper and Lower Tempest Sandstone. Figure modified from Cody et al. [2].

### 5.5. Regional Comparison

When the detrital zircon data are evaluated more regionally, a noteworthy provenance difference is seen in comparing results from wells in the Central Ridge and southern Flemish Pass area (South Tempest G-88, Panther P-52 and Lancaster G-70) against results from the northern Flemish Pass region (Baccalieu I-78). Firstly, the Iberian-related Permian–Carboniferous zircons are only seen in samples from the Panther P-52, South Tempest G-88 and Lancaster G-70 wells, but not in samples from the Baccalieu I-78 well. This suggests the Iberian influence was only present in the Central Ridge and southern Flemish Pass area, but not the northern Flemish Pass. Additionally, the Cambrian–Devonian-aged grains are much more significant in samples from the Baccalieu I-78 well than in samples from the other three wells, indicating the Central Mobile Belt was more of a minor sediment source for wells in the Central Ridge and Southern Flemish Pass areas during the Upper Jurassic. These two observations are important as it suggests that northern areas of the basin are more likely to see detritus from the northeast or west, with the Central Mobile Belt representing a major sediment source, whereas the Central Ridge and southern Flemish Pass Basin is more likely to have detritus that was derived from the east from Iberian-related rocks.

### 5.6. Constraints on Depositional Ages

The three Jurassic zircon grains ( $145 \pm 5$  Ma,  $148 \pm 4$  Ma,  $150 \pm 6$  Ma) from the Upper Tempest Sandstone sample (Panther P-52 (3210 m)) can help refine the depositional age of this unit (Figure 13). In this sample, the weighted average of age dates from these three grains is  $147.5 \pm 2.8$  Ma (MSWD = 0.85), which may be taken as the maximum depositional age [72]. If the age of the youngest single grain is accepted, the maximum depositional age would be reduced to  $144.9 \pm 5.6$  Ma. Whether the youngest single grain or the weighted average of the three grains is used, a Late Tithonian depositional age for the Upper Tempest Sandstone is suggested, as the Tithonian Stage ranges from  $152.1 \pm 0.9$  to  $\sim 145$  Ma [73].

When compared to biostratigraphic interpretations for this interval, a Late Tithonian age is consistent with findings from Robertson Research [74] but conflicts with interpretations from Bujak Davies Group [75] who interpreted this interval to be Early Kimmeridgian in age. Based on the detrital zircon age results, and Robertson Research [74], the Upper Tempest Sandstone from the Panther P-52 well is considered to have a Late Tithonian depositional age. As cuttings were used for this sample, there is a possibility that caving occurred (material from previously penetrated beds up section in the well) and potentially contaminated this sample with younger detrital zircons from above. However, given the presence of multiple Upper Jurassic grains in this sample and the absence of any Cretaceous or younger grains, it is improbable they originated from cavings.

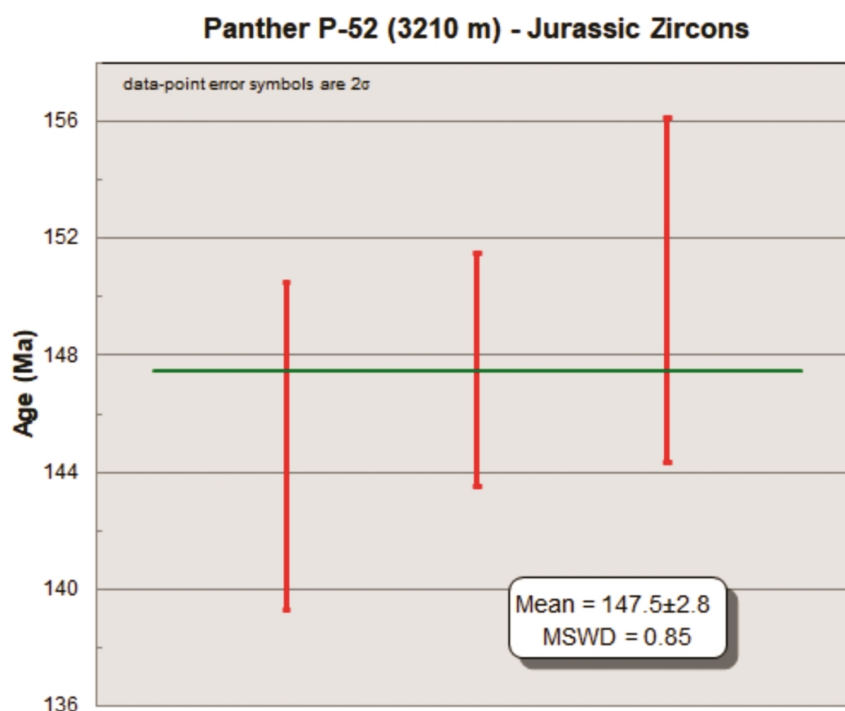


**Figure 13.**  $^{238}\text{U}/^{206}\text{Pb}$  ages of the three youngest detrital zircons (represented by red lines) from the Upper Tempest Sandstone sample from the Panther P-52 well. Weighted average of these three Jurassic grains (shown by green line) is  $147.5 \pm 2.8$  Ma (MSWD = 0.85), which may be taken as the maximum depositional age [72].

### 5.7. Significance of Heavy Mineral Assemblages

Detrital heavy mineral assemblages in cuttings samples from the Upper Jurassic sandstones and mudstones are dominated by either rutile + zircon + apatite ± chromite or rutile + apatite + tourmaline, with minor zircon. These are among the most stable heavy minerals surviving burial diagenesis [76] suggesting that less stable detrital heavy minerals (olivine, pyroxene, amphibole) may have been lost preferentially during diagenesis of these units. Detrital apatite may be preferentially dissolved in acidic groundwaters during transport or alluvial storage on floodplains of major rivers in humid tropical climates [43], suggesting that apatite-bearing detritus was transported under arid temperate conditions or stored/recycled to only limited extents.

Rutile occurs in a large range of medium- to high-grade metamorphic rocks and particular kinds of igneous rocks (e.g., quartz veins, alkalic granites, pegmatites, carbonates, kimberlites, metasomatised peridotites) as well as detrital grains in sediments and sedimentary rocks [77]. Apatite, tourmaline and zircon are common in many of the same

lithologies as well as a wide range of granitic rocks; chromite is particularly abundant in mafic and ultramafic rocks. Thus, it is likely that the detrital source terranes of the sedimentary units of this study contained diverse lithologies. This is consistent with the whole rock Th/Sc–Zr/Sc ratios of the Upper Jurassic sandstones and mudstones units being similar to the composition of average upper continental crust (Figure 3).

## 6. Conclusions

Often, less focus is shown to finer-grained intervals in detrital mineral provenance studies as it is predicted that there will not be enough heavy mineral grains large enough to separate and analyze. Results of this study demonstrate the utility and effectiveness of MLA/SEM techniques combined with LA-ICP-MS for fine-grained sedimentary rocks. Detailed analysis of Upper Jurassic rocks from the Flemish Pass Basin and Central Ridge through a combination of detrital zircon U-Pb geochronology, whole rock geochemistry and heavy mineral analysis highlights important provenance characteristics of these units. Whole rock geochemistry was employed on both Upper Jurassic sandstones and mudstones to identify sediment provenance. Whole rock Th/Sc–Zr/Sc systematics indicate that the units were derived from sediment sources with upper crustal compositions, commonly seen in passive margins, with significant zircon recycling. In addition, detrital zircon geochronology revealed significant information for generating provenance and paleodrainage models. Zircon populations indicate grains from most units were likely derived from the Avalon Zone, Central Mobile Belt, and underlying basement. A significant population of Permian–Carboniferous grains, however, are present in a few samples suggesting derivation from Iberian intrusive rocks.

In addition to important provenance information, Upper Jurassic detrital zircons constrain the age of the Upper Tempest Sandstone to Late Tithonian or younger. This is a particularly useful result as conflicting ages exist in the published biostratigraphic interpretations for this unit.

**Supplementary Materials:** The following are available online at <https://www.mdpi.com/2075-163X/11/3/265/s1>, Table S1: Heavy Mineral Abundances determined by MLA-SEM for Sandstone and Mudstone from the Flemish Pass Basin and Central Ridge, offshore Newfoundland, Canada, Table S2A: Detrital Zircon U-Pb LA-ICP-MS Data for Sandstone and Mudstone from the Flemish Pass Basin and Central Ridge, offshore Newfoundland Canada, Table S2B: U-Pb LA-ICP-MS Data for Zircon Reference Materials, Table S3: X-ray Fluorescence Major Element Data for Sandstone and Mudstone from the Flemish Pass Basin and Central Ridge, offshore Newfoundland Canada, Table S4: X-ray Fluorescence Minor/Trace Element Data for Sandstone and Mudstone from the Flemish Pass Basin and Central Ridge, offshore Newfoundland Canada, Table S5: HF/HNO<sub>3</sub> Acid Digestion ICP-MS Trace Element Data for Sandstone and Mudstone from the Flemish Pass Basin and Central Ridge, offshore Newfoundland Canada, Table S6: Na<sub>2</sub>O<sub>2</sub> Sinter Digestion ICP-MS Trace Element Data for Sandstone and Mudstone from the Flemish Pass Basin and Central Ridge, offshore Newfoundland Canada.

**Author Contributions:** M.S. completed analytical work as part of a MSc thesis at Memorial University. The project was conceptualized by P.J.S. and the whole project was supervised by P.J.S.; D.H.C.W.; M.S. completed the majority of writing and conversion of the MSc thesis to this manuscript with input from P.J.S. and D.H.C.W. All authors have read and agreed to the published version of the manuscript.

**Funding:** This research was funded by the Mitacs-Accelerate Graduate Research Internship Program and Suncor Energy Inc, grant number IT03082 to P.J.S.

**Institutional Review Board Statement:** Not applicable.

**Acknowledgments:** We would like to thank those working at the CREAT Network at Memorial University. Dylan Goudie, David Grant, Sarah Jantzi, and Pam King were extremely helpful with guidance and timely analyses for the various methods undertaken. Kate Souders and Angela Norman helped significantly by teaching M.S. sample preparation methods as well as aiding with analytical techniques.

**Conflicts of Interest:** The authors declare no conflict of interest.

## References

1. Lowe, D.G.; Sylvester, P.J.; Enachescu, M.E. Provenance and Paleodrainage Patterns of Upper Jurassic and Lower Cretaceous Synrift Sandstones in the Flemish Pass Basin, Offshore Newfoundland, East Coast of Canada. *Bull. Am. Assoc. Pet. Geol.* **2011**, *95*, 1295–1320. [CrossRef]
2. Cody, J.; Hunter, D.; Schwartz, S.; Marshall, J.; Haynes, S.; Gruschwitz, K.; McDonough, M. A Late Jurassic play fairway beyond the Jeanne d’Arc Basin: New insights for a petroleum system in the Northern Flemish Pass Basin. In *New Understanding of the Petroleum Systems of Continental Margins of the World: 32nd Annual, Canada, 19–22, August, 2018*; Rosen, N.C., Weimer, P., Coutes dos Anjos, S.M., Henrickson, S., Marques, E., Mayall, M., Fillon, R., D’Agostino, T., Saller, A., Campion, K., et al., Eds.; Society of Economic Paleontologists and Mineralogists: Tulsa, OK, USA, 2012; ISBN 978-0-9836097-8-0.
3. Fowler, M.G.; Obermajer, M.; Achal, S.; Milovic, M. *Results of Geochemical Analyses of an Oil Sample from Mizzen L-11 Well, Flemish Pass, Offshore Eastern Canada*; Geological Survey of Canada Paper: Ottawa, ON, Canada, 2007.
4. Canada-Newfoundland and Labrador Offshore Petroleum Board (C-NLOPB). Schedule of Wells–Newfoundland and Labrador Offshore Area. Lancaster G-70, Panther P-52, South Tempest G-88, North Dana I-43. 2007. Available online: <https://www.cnlopb.ca/wells/> (accessed on 12 January 2021).
5. Canada-Newfoundland and Labrador Offshore Petroleum Board (C-NLOPB). Schedule of Wells–Newfoundland and Labrador Offshore Area. Baccaieu I-78. 2011. Available online: <https://www.cnlopb.ca/wells/> (accessed on 12 January 2021).
6. McCracken, J.N.; Haager, A.; Saunders, K.I.; Veilleux, B.W. Late Jurassic source rocks in the northern Flemish Pass Basin, Grand Banks of Newfoundland. In *Proceedings of the GeoCanada 2000, Calgary, AB, Canada, 29 May–2 June 2000*; Volume 25.
7. Creaney, S.; Allison, B.H. An organic geochemical model of oil generation in the Avalon/Flemish Pass Sub-basins, East Coast Canada. *Bull. Can. Pet. Geol.* **1987**, *35*, 12–23.
8. Sinclair, I.K. Evolution of Mesozoic-Cenozoic sedimentary basins in the Grand Banks area of Newfoundland and comparison with Flavy’s (1974) rift model. *Bull. Can. Pet. Geol.* **1988**, *34*, 255–273.
9. McAlpine, K.D. *Mesozoic Stratigraphy, Sedimentary Evolution, and Petroleum Potential of the Jeanne d’Arc Basin, Grand Banks of Newfoundland*; Geological Survey of Canada Paper: Ottawa, ON, Canada, 1990; ISBN 978-0-660-13725-4.
10. DeSilva, N. Submarine fans on the northeastern Grand Banks, offshore Newfoundland. In *Proceedings of the GCSSEPM Foundation 15th Annual Research Conference—Submarine Fans and Turbidite Systems, Houston, TX, USA, 4–7 December 1994*; pp. 95–104.
11. Enachescu, M.E. Tectonic and structural framework of the northeast Newfoundland continental margin. In *Sedimentary Basins and Basin Forming Mechanisms*; Beaumont, C., Tankard, A.J., Eds.; Canadian Society of Petroleum Geologists: Calgary, AB, Canada, 1987; pp. 117–146.
12. Sharp, I.R.; Higgins, H.; Scott, M.; Freitag, U.; Allsop, C.; Kane, K.; Sultan, A.; Doubleday, P.; Leppard, C.; Bloomfield, J.; et al. Rift to drift evolution and hyper-extension in the North Atlantic—insights from a super-regional approach. In *Extended Abstracts: 6th Conjugate Margins Conference, Halifax, NS, Canada, 19–22 August 2018*; Dalhousie University: Halifax, NS, Canada, 2019; ISBN 0-9810595-8.
13. Enachescu, M.E. Extended basement beneath the intracratonic rifted basins of the Grand Banks of Newfoundland. *Can. J. Explor. Geophys.* **1988**, *24*, 48–65.
14. Tankard, A.J.; Welsink, H.J. Extensional tectonics and stratigraphy of Hibernia oil field, Grand Banks, Newfoundland. *Bull. Am. Assoc. Pet. Geol.* **1987**, *71*, 1210–1232.
15. Foster, D.G.; Robinson, A.G. Geological history of the Flemish Pass Basin, offshore Newfoundland. *Bull. Am. Assoc. Pet. Geol.* **1993**, *77*, 588–609.
16. Desilva, N. Flemish Pass Basin: Hydrocarbon prospectivity and potential deep-water development. *J. Can. Pet. Technol.* **2000**, *39*, 22–25. [CrossRef]
17. Enachescu, M.E.; Hogg, J.R. Exploring for Atlantic Canada’s next giant petroleum discovery. *CSEG Rec.* **2005**, *30*, 19–30.
18. Enachescu, M.E. *Call for Bids NL06-1, Parcels 1, 2 and 3, Regional Setting and Petroleum Geology Evaluation*; Government of Newfoundland Department of Natural Resources: St. John’s, NL, Canada, 2006.
19. Canada-Newfoundland and Labrador Offshore Petroleum Board (C-NLOPB). Petroleum Reserves and Resources Newfoundland Offshore Area 2020. Available online: <https://www.cnlopb.ca/resource/information/> (accessed on 18 November 2020).
20. McDonough, M.; Richardsen, G.; Haynes, S.; Minielly, G.; Gruschwitz, K.; Thorpe, G.; Anfort, S. Paradigm Shift in East Coast Canada: The Lightning of Flemish Pass Oil. In *NGF Abstracts and Proceedings of the Geological Society of Norway, Tromsø, Norway, 2–6 June 2014*; Norsk Geologisk Forening: Trondheim, Norway, 2014.
21. Enachescu, M.E. *Petroleum Exploration Opportunities in the Flemish Pass Basin, Newfoundland and Labrador Offshore Area; Call for Bids NL13-01, Area “C”—Flemish Pass Basin, Parcel 1*; Government of Newfoundland Department of Natural Resources: St. John’s, NL, Canada, 2014.
22. Nelson, T.A. Density Separation of Clay Minerals. Master’s Thesis, Oregon State University, Corvallis, OR, USA, 1971.
23. Schieber, J.; Zimmerle, W. Petrography of shales: A survey of techniques. In *Shales and Mudstones. Petrography, Petrophysics, Geochemistry and Economic Geology*; Schieber, J., Zimmerle, W., Sethi, P., Eds.; Schweizerbart: Stuttgart, Germany, 1998; Volume 2, pp. 3–12.

24. Sylvester, P.J. *Use of the Mineral Liberation Analyzer (MLA) for Mineralogical Studies of Sediments and Sedimentary Rocks*; Mineralogical Association of Canada Short Course 42; Memorial University: St. John's, NL, Canada, 2012; pp. 1–16.
25. Morad, S. SEM study of authigenic rutile, anatase and brookite in Proterozoic sandstones from Sweden. *Sediment. Geol.* **1986**, *46*, 77–89. [[CrossRef](#)]
26. Pe-Piper, G.; Karim, A.; Piper, D.J.W. Authigenesis of Titanite Minerals and the Mobility of Ti: New Evidence from Pro-Deltaic Sandstones, Cretaceous Scotian Basin, Canada. *J. Sediment. Res.* **2011**, *81*, 762–773. [[CrossRef](#)]
27. Pe-Piper, G.; Weir-Murphy, S. Early Diagenesis of Inner-Shelf Phosphorite and Iron-Silicate Minerals, Lower Cretaceous of the Orpheus Graben, Southeastern Canada: Implications for the Origin of Chlorite Rims. *Bull. Am. Assoc. Pet. Geol.* **2008**, *92*, 1153–1168. [[CrossRef](#)]
28. Paton, C.; Hellstrom, J.; Paul, B.; Woodhead, J.; Hergt, J. Iolite: Freeware for the visualisation and processing of mass spectrometer data. *J. Anal. At. Spectrom.* **2011**, *26*, 2508–2518. [[CrossRef](#)]
29. Petrus, J.A.; Kamber, B.S. VizualAge: A Novel Approach to Laser Ablation ICP-MS U-Pb Geochronology Data Reduction. *Geostand. Geoanal. Res.* **2012**, *36*, 247–270. [[CrossRef](#)]
30. Andersen, T. Correction of Common Lead in U-Pb Analyses That Do Not Report  $^{204}\text{Pb}$ . *Chem. Geol.* **2002**, *192*, 59–79. [[CrossRef](#)]
31. Wiedenbeck, M.; Allé, P.; Corfu, F.; Griffin, W.; Meier, M.; Oberli, F.; Quadt, A.V.; Roddick, J.; Spiegel, W. Three natural zircon standards for U-Th-Pb, Lu-Hf, trace element and REE analyses. *Geostand. Newsl.* **1995**, *19*, 1–23. [[CrossRef](#)]
32. Jaffey, A.H.; Flynn, K.F.; Glendenin, L.E.; Bentley, W.C.; Essling, A.M. Precision measurement of half-lives and specific activities of  $^{235}\text{U}$  and  $^{238}\text{U}$ . *Phys. Rev. C* **1971**, *4*, 1889–1906. [[CrossRef](#)]
33. Ludwig, K.R. *User's Manual for Isoplot 3.75: A Geochronological Toolkit for Microsoft Excel*; Berkeley Geochronology Center Special Publication; Berkeley Geochronological Center: Berkeley, CA, USA, 2012; Available online: [http://www.bgc.org/isoplot\\_etc/isoplot/Isoplot3\\_75-4\\_15manual.pdf](http://www.bgc.org/isoplot_etc/isoplot/Isoplot3_75-4_15manual.pdf) (accessed on 18 November 2020).
34. Ketchum, J.W.; Jackson, S.E.; Culshaw, N.G.; Barr, S.M. Depositional and tectonic setting of the Paleoproterozoic Lower Aillik Group, Makkovik Province, Canada: Evolution of a passive margin-foredeep sequence based on petrochemistry and U-Pb (TIMS and LAM-ICP-MS) geochronology. *Precambrian Res.* **2001**, *105*, 331–356. [[CrossRef](#)]
35. Sláma, J.; Košler, J.; Condon, D.J.; Crowley, J.L.; Gerdes, A.; Hanchar, J.M.; Horstwood, M.S.; Morris, G.A.; Nasdala, L.; Norberg, N.; et al. Plešovice zircon—A new natural reference material for U-Pb and Hf isotopic microanalysis. *Chem. Geol.* **2008**, *249*, 1–35. [[CrossRef](#)]
36. Stern, R.A.; Bodorkos, S.; Kamo, S.L.; Hickman, A.H.; Corfu, F. Measurement of SIMS instrumental mass fractionation of Pb isotopes during zircon dating. *Geostand. Geoanal. Res.* **2009**, *33*, 145–168. [[CrossRef](#)]
37. Fedo, C.M.; Sircombe, K.N.; Rainbird, R.H. Detrital Zircon Analysis of the Sedimentary Record. In *Zircon: Experiments, Isotopes, and Trace Element Investigations*; Hanchar, J.M., Hoskin, P., Eds.; Mineralogical Society of America: Chantilly, VA, USA, 2003; Volume 53, pp. 277–303.
38. Dodson, M.H.; Compston, W.; Williams, I.S.; Wilson, J.F. A search for ancient detrital zircons in Zimbabwean sediments. *J. Geol. Soc. Lond.* **1988**, *145*, 977–983. [[CrossRef](#)]
39. Vermeesch, P. How Many Grains Are Needed for a Provenance Study? *Earth Planet. Sci. Lett.* **2004**, *224*, 441–451. [[CrossRef](#)]
40. Jenner, G.A.; Longerich, H.P.; Jackson, S.E.; Fryer, B.J. ICP-MS—a powerful tool for high precision trace element analyses in earth sciences: Evidence from analyses of selected U.S.G.S. reference samples. *Chem. Geol.* **1990**, *83*, 105–118. [[CrossRef](#)]
41. McLennan, S.M.; Bock, B.; Hemming, S.R.; Hurowitz, J.A.; Lev, S.M.; McDaniel, D.K. The roles of provenance and sedimentary processes in the geochemistry of sedimentary rocks. In *Geochemistry of Sediments and Sedimentary Rocks: Evolutionary Considerations to Mineral Deposit-Forming Environments*; Lentz, D.R., Ed.; GeoText 4; Geological Association of Canada: St. John's, NL, Canada, 2003; pp. 7–38.
42. McLennan, S.M.; Taylor, S.R.; McCulloch, M.T.; Maynard, J.B. Geochemical and Nd-Sr Isotopic Composition of Deep-Sea Turbidites: Crustal Evolution and Plate Tectonic Associations. *Geochim. Cosmochim. Acta* **1990**, *54*, 2015–2050. [[CrossRef](#)]
43. Morton, A.C.; Hallsworth, C.R. Identifying provenance-specific features of detrital heavy mineral assemblages in sandstones. *Sediment. Geol.* **1994**, *90*, 241–256. [[CrossRef](#)]
44. Morton, A.C.; Hallsworth, C.R. Processes controlling the composition of heavy mineral assemblages in sandstones. *Sediment. Geol.* **1999**, *124*, 3–30. [[CrossRef](#)]
45. Hallsworth, C.R.; Morton, A.C.; Claoue-Long, J.; Fanning, C.M. Carboniferous sand provenance in the Pennine Basin, UK; constraints from heavy mineral and detrital zircon age data. *Sediment. Geol.* **2000**, *137*, 147–185. [[CrossRef](#)]
46. Morton, A.C.; Knox, R.W.O.B.; Hallsworth, C.R. Correlation of reservoir sandstones using quantitative heavy mineral analysis. *Pet. Geosci.* **2002**, *8*, 251–262. [[CrossRef](#)]
47. Morton, A.C.; Whitham, A.G.; Fanning, C.M. Provenance of Late Cretaceous to Paleocene submarine fan sandstones in the Norwegian Sea; integration of heavy mineral, mineral chemical and zircon age data. *Sediment. Geol.* **2005**, *182*, 3–28. [[CrossRef](#)]
48. Totten, M.W.; Hanan, M.A. Heavy minerals in shales. In *Heavy Minerals in Use, Developments in Sedimentology*; Mange, M., Wright, D.T., Eds.; Elsevier: Amsterdam, The Netherlands, 2007; Volume 58, pp. 323–341; ISBN 978-0-444-51753-1.
49. Macquaker, J.H.S.; Adams, A.E. Maximizing information from fine-grained sedimentary rocks: An inclusive nomenclature for mudstones. *J. Sediment. Res.* **2003**, *73*, 735–744. [[CrossRef](#)]
50. Rubey, W.W. The size distribution of heavy minerals within a water-laid sandstone. *J. Sediment. Petrol.* **1933**, *3*, 3–29.

51. Hubert, J.F. A zircon-tourmaline-rutile maturity index and the interdependence of the composition of heavy mineral assemblages with the gross composition and texture of sandstones. *J. Sediment. Petrol.* **1962**, *32*, 440–450.
52. Morton, A.C. Depth control of intrastratal solution of heavy minerals from the Palaeocene of the North Sea. *J. Sediment. Petrol.* **1979**, *49*, 281–286.
53. Smale, D.; Morton, A.C. Heavy mineral suites of core samples from the McKee Formation (Eocene-lower Oligocene), Taranaki; implications for provenance and diagenesis. *N. Z. J. Geol. Geophys.* **1987**, *30*, 299–306. [[CrossRef](#)]
54. Milliken, K.L. Loss of provenance information through subsurface diagenesis in Plio-Pleistocene sandstones, northern Gulf of Mexico. *J. Sediment. Petrol.* **1988**, *58*, 992–1002.
55. Robertson Research International Ltd. Stratigraphic Correlation of Baccaieu I-78, Gabriel C-60, Lancaster G-70, and South Tempest G-88 Wells. Robertson Research International Limited Report Number 6268. 2002. Available online: [https://basin.gdr.nrcan.gc.ca/wells/index\\_e.php](https://basin.gdr.nrcan.gc.ca/wells/index_e.php) (accessed on 18 November 2020).
56. Jenkins, W.A.M. Palynology of the Lancaster F-70 (G-70) Well. Flemish Pass, Offshore Newfoundland. Associated Biostratigraphic Consultants, Calgary. December 1986. Available online: [https://basin.gdr.nrcan.gc.ca/wells/index\\_e.php](https://basin.gdr.nrcan.gc.ca/wells/index_e.php) (accessed on 18 November 2020).
57. BP Exploration Canada Ltd. *Biostratigraphic Study of Flemish Pass Wells*. 1991. Available online: [https://basin.gdr.nrcan.gc.ca/wells/index\\_e.php](https://basin.gdr.nrcan.gc.ca/wells/index_e.php) (accessed on 18 November 2020).
58. Pollock, J.C.; Hibbard, J.P.; Sylvester, P.J. Early Ordovician Rifting of Avalonia and Birth of the Rheic Ocean: U–Pb Detrital Zircon Constraints from Newfoundland. *J. Geol. Soc.* **2009**, *166*, 501–515. [[CrossRef](#)]
59. Willner, A.P.; Gerdes, A.; Massonne, H.-J.; van Staal, C.R.; Zagorevski, A. Crustal Evolution of the Northeast Laurentian Margin and the Peri-Gondwanan Microcontinent Ganderia Prior to and During Closure of the Iapetus Ocean: Detrital Zircon U–Pb and Hf Isotope Evidence from Newfoundland. *Geosci. Can.* **2014**, *41*, 345–364. [[CrossRef](#)]
60. Kerr, A.; Jenner, G.A.; Fryer, B.J. Sm–Nd Isotopic Geochemistry of Precambrian to Paleozoic Granitoid Suites and the Deep-Crustal Structure of the Southeast Margin of the Newfoundland Appalachians. *Can. J. Earth Sci.* **1995**, *32*, 224–245. [[CrossRef](#)]
61. Murphy, J.B.; Keppie, J.D.; Dostal, J.; Cousins, B.L. Repeated late Neoproterozoic–Silurian lower crustal melting beneath the Antigonish Highlands, Nova Scotia: Nd isotopic evidence and tectonic interpretations. In *Avalonian and Related Peri-Gondwanan Terranes of the Circum-North Atlantic*; Nance, R.D., Thompson, M.D., Eds.; Special Papers; Geological Society of America: Boulder, CO, USA, 1996; Volume 304, pp. 109–120.
62. Bevier, M.L.; Barr, S.M. U–Pb age constraints on the stratigraphy and tectonic history of the Avalon terrane, New Brunswick, Canada. *J. Geol.* **1990**, *58*, 53–63. [[CrossRef](#)]
63. Zartman, O.; Hermes, D. Archean inheritance in zircon from late Paleozoic granites from the Avalon zone of southeastern New England: An African connection. *Earth Planet. Sci. Lett.* **1987**, *82*, 305–315. [[CrossRef](#)]
64. King, L.H.; Fader, G.B.J.; Jenkins, W.A.M.; King, E.L. Occurrence and Regional Geological Setting of Paleozoic Rocks on the Grand Banks of Newfoundland. *Can. J. Earth Sci.* **1986**, *23*, 504–526. [[CrossRef](#)]
65. Bell, J.S.; Howie, R.D. Paleozoic Geology. In *Geology of the Continental Margin of Eastern Canada*; Keen, M.J., Williams, G.L., Eds.; Geological Survey of Canada: Ottawa, ON, Canada, 1990; pp. 141–165.
66. Sylvester, P.J. Mineralogy and provenance of Carboniferous sandstone and shale units in the Deer Lake and Bay St. George Basins, western Newfoundland. Government of Newfoundland and Labrador, PEEP (Petroleum Exploration Enhancement Project) Workshop Presentation 2012. Available online: <https://www.gov.nl.ca/iet/energy/petroleum/onshore/peep/> (accessed on 2 April 2014).
67. Nauton-Fourteu, M.; Tyrrell, S.; Morton, A.; Mark, C.; O’Sullivan, G.J.; Chew, D.M. Constraining Recycled Detritus in Quartz-Rich Sandstones: Insights from a Multi-Proxy Provenance Study of the Mid-Carboniferous, Clare Basin, Western Ireland. *Basin Res.* **2021**, *33*, 342–363. [[CrossRef](#)]
68. King, L.H.; Fader, G.B.; Poole, W.H.; Wanless, R.K. Geological Setting and Age of the Flemish Cap Granodiorite, East of the Grand Banks of Newfoundland. *Can. J. Earth Sci.* **1985**, *22*, 1286–1298. [[CrossRef](#)]
69. Kerr, A.; Dunning, G.R.; Tucker, R.D. The Youngest Paleozoic Plutonism of the Newfoundland Appalachians: U–Pb Ages from the St. Lawrence and François Granites. *Can. J. Earth Sci.* **1993**, *30*, 2328–2333. [[CrossRef](#)]
70. Priem, H.N.A.; Den Tex, E. Tracing crustal evolution in the NW Iberian Peninsula through the Rb–Sr and U–Pb systematics of Paleozoic granitoids: A review. *Phys. Earth Planet. Inter.* **1984**, *35*, 121–130. [[CrossRef](#)]
71. Hiscott, R.N.; Marsaglia, K.M.; Wilson, R.C.L.; Robertson, A.H.F.; Karner, G.D.; Tucholke, B.E.; Pletsch, T.; Petschick, R. Detrital Sources and Sediment Delivery to the Early Post-Rift (Albian–Cenomanian) Newfoundland Basin East of the Grand Banks: Results from ODP Leg 210. *Bull. Can. Pet. Geol.* **2007**, *56*, 69–92. [[CrossRef](#)]
72. Dickinson, W.R.; Gehrels, G.E. Use of U–Pb Ages of Detrital Zircons to Infer Maximum Depositional Ages of Strata: A Test against a Colorado Plateau Mesozoic Database. *Earth Planet. Sci. Lett.* **2009**, *288*, 115–125. [[CrossRef](#)]
73. Cohen, K.M.; Finney, S.C.; Gibbard, P.L.; Fan, J.-X. The ICS International Chronostratigraphic Chart. *Episodes* **2013**, *36*, 199–204. [[CrossRef](#)] [[PubMed](#)]
74. Robertson Research International Ltd. Palynology (2650–4205 m) and Micropaleontology (2635–4210 m), Panther P-52 Biostratigraphy Report. 2004. Available online: [https://basin.gdr.nrcan.gc.ca/wells/index\\_e.php](https://basin.gdr.nrcan.gc.ca/wells/index_e.php) (accessed on 18 November 2020).

- 
75. Bujak Davies Group. Palynological biostratigraphy of the interval 395–4203 m, Panther P-52, Grand Banks. Geological Survey of Canada Open File Report 1876. 1987. Available online: [https://basin.gdr.nrcan.gc.ca/wells/index\\_e.php](https://basin.gdr.nrcan.gc.ca/wells/index_e.php) (accessed on 18 November 2020).
  76. Morton, A.C.; Hallsworth, C.R. Stability of Detrital Heavy Minerals During Burial Diagenesis. In *Heavy Minerals in Use, Developments in Sedimentology*; Mange, M., Wright, D.T., Eds.; Elsevier: Amsterdam, The Netherlands, 2007; Volume 58, pp. 215–245; ISBN 978-0-444-51753-1.
  77. Meinhold, G. Rutile and Its Applications in Earth Sciences. *Earth Sci. Rev.* **2010**, *102*, 1–28. [[CrossRef](#)]